Reviews

Review of the Structure and Processing-Defect-Property Relationships of Potassium Titanyl Phosphate: A Strategy for Novel Thin-Film Photonic Devices

Michael E. Hagerman and Kenneth R. Poeppelmeier*

Department of Chemistry, Northwestern University, Evanston, Illinois 60208

Received October 25, 1994. Revised Manuscript Received February 17, 1995[⊗]

Potassium titanyl phosphate ($KTiOPO_4$ or KTP) is a premier nonlinear optical (NLO) material. KTP has a waveguide figure-of-merit which is twice that of other mixed metal oxides and is unparalleled at the doubling of Nd laser radiation near 1 μm. It has a complex high-temperature chemistry that produces a dramatic effect upon the observed nonlinear optical behavior. A summary is provided of the current knowledge of the single-crystal $KTiOPO_4$ structure field with specific focus on defect chemistry, structure, and processing-defect-property relationships and waveguide technology. On the basis of this summary, a strategy is proposed for the development of novel electrooptical and nonlinear optical devices based on thin-film fabrication.

1. Background

The majority of NLO materials currently used in devices are fabricated from bulk single crystals. Optimum properties for optical quality, such as transparency, efficiency, phase-matching, high fluence stability, mechanical integrity, and chemical stability, which should ideally all coexist, place stringent limits on the number of useful NLO materials.[1] It is the goal of this review to summarize the existing knowledge of the defect chemistry, structure and processing-defect-property relationships, and waveguide technology in single-crystal KTP in order to develop a better understanding of the processing techniques and conditions required to produce high-quality KTP thin films with potential nonlinear optical and electrooptical device applications. Owing to the structural properties of KTP, it has been possible to design and synthesize a large structure field to fine tune and modify desired nonlinear and electrooptical properties.[2] Consequently, it has been observed that the properties of interest for applications of crystalline nonlinear optical mixed-metal oxides are often determined by the defect structures introduced in the materials as a result of the various processing procedures used to produce bulk crystals, waveguide devices and thin films.[3] Therefore, it is extremely important that we continue to develop our understanding of the complex chemistry of this unique and remarkably applicable NLO material. The successful fabrication of waveguides based on thin films of KTP and related isomorphs for use in integrated optical devices will undoubtedly depend on a coherent and unified application of fundamental chemical and physical principles.

1.1. Structure. The structure of KTP was first determined by Tordjman et al.[4] KTP crystallizes in the noncentrosymmetric orthorhombic space group $Pna2_1$ with the lattice parameters $a = 12.814(6)$ Å, $b = 6.404(2)$ Å, and $c = 10.616(5)$ Å. The structure is characterized by helical chains of TiO_6 octahedra that are linked at two corners and are separated by PO_4 tetrahedra (Figure 1.1). Alternating long and short Ti-O bonds occur along these chains that result in a net c-directed polarization and are the major contributors to the large nonlinear optic and electrooptic coefficients (Figure 1.2).[5] There are 10 inequivalent oxygen sites per unit cell (eight Ti-O-P bonds and two Ti-O-Ti bonds). The potassium ion is located in a high coordination number site and is bonded to the oxygen atoms in the TiO_6 octahedra and the PO_4 tetrahedra. Channels exist along the c axis ([001] direction), whereby potassium ions can diffuse via a vacancy mechanism.[6] The influence of cation diffusion through these channels on ionic conductivity, ferroelectricity, and damage mechanisms will be discussed in sections 2 and 3. Several derivatives of KTP have been synthesized through ion exchange of potassium in these channels. Consequently, waveguide structures based on KTP crystals have been fabricated through ion-exchange techniques; see section 4.

1.2. Crystal Growth. KTP was first synthesized in 1890 by Ouvrard using molten potassium pyrophos-

* To whom correspondence should be addressed.

[⊗] Abstract published in *Advance ACS Abstracts,* April 1, 1995.

(1) Jacco, J. C. *SPIE Int. Soc. Opt. Eng.* **1988**, *968*, 93.
(2) Stucky, G. D.; Phillips, M. L. F.; Gier, T. E. *Chem. Mater.* **1989**, *1*, 492.
(3) Morris, P. A. *Solid State Optical Materials*; Bruce, A. J., Hiremath, B. V., Eds.; American Ceramic Society: Ohio, 1992; Ceramic Transactions, Vol. 28, p 467.
(4) Tordjman, P. I.; Masse, R.; Guitel, J. C. *Z. Kristallogr.* **1974**, *139*, 103.
(5) Bierlein, J. D.; Vanherzeele, H. *J. Opt. Soc. Am. B.* **1989**, *6*, 622.
(6) Bierlein, J. D. *SPIE Int. Soc. Opt. Eng.* **1989**, *1104*, 2.

0897-4756/95/2807-0602$09.00/0 © 1995 American Chemical Society

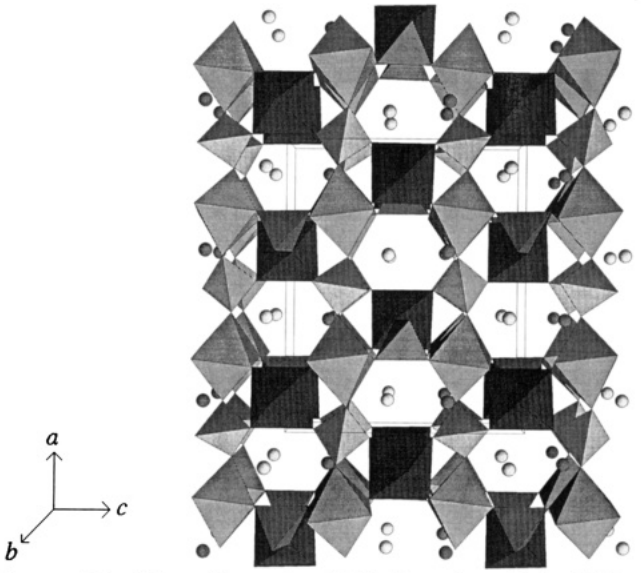

Figure 1.1. View down the [010] direction of the KTP structure: the spheres represent K cations, the octahedra represent TiO_6 anionic groups, and the tetrahedra represent PO_4 anionic groups. All of the vertices are oxygen atoms.

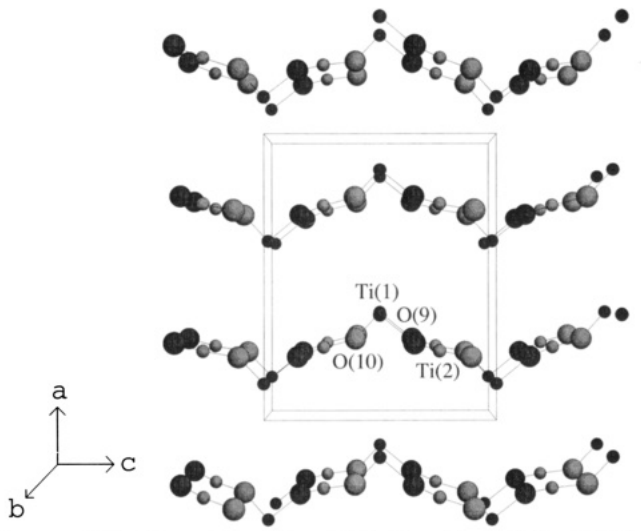

Figure 1.2. View down the [010] direction of the KTP structure: Ti(1)−O(9)−Ti(2)−O(10) network of alternating short and long bonds.

phate and orthophosphate fluxes.[7] KTP melts incongruently (near 1150 °C), and therefore normal melt processes cannot be used for crystal growth. Two KTP synthesis methods are in general use, anhydrous flux growth as described by Loiacono and co-workers[8] and by Ballman,[9] and moderately high-temperature hydrothermal growth as perfected by Belt et al.[10] and Laudise and co-workers.[11] The chosen method for crystal growth can have a dramatic effect on crystal quality, purity, and observed properties. Patents by Bierlein and Gier delineate flux and hydrothermal crystal growths and the use of KTP as an NLO device.[1] The preferred method involved cooling a hydrothermal flux of potassium salts and TiO_2 from 850 to 650 °C over a period of a week.[12] The solution was contained in a gold tube that was pressurized to 3000 atm. An alternative method utilized TiO_2 nutrients or seeds transported through a temperature gradient of 10 °C/in. from 700 to 500 °C.[13] Small KTP crystals can also be used as seeds for crystal growth. The geometrical domain and morphology of the crystal are related to the orientation of the seed crystal used.[14] Bolt has examined the relation between crystal structure and morphology in KTP.[15] Bierlein has noted the following range of conditions for hydrothermal $KTiOPO_4$ crystallization: 500−800 °C temperature, K/P ratio ranging from 0.8−1.5, and a flux composed of 0.7−1.0 g of KH_2PO_4/cm^3 H_2O.[16] The phase relations and solubility of KTP have been previously described in detail by Laudise et al.[13] and Loiacono et al.[17]

Hydrothermal growth of KTP crystals in a size and quality useful for optical applications required many weeks of high-temperature growth. In contrast, the use of high-temperature molten fluxes and high-pressure aqueous solvents limited the size and quality of the crystals.[10] As a result, low-temperature, low-pressure conditions have been examined.[18] Belt reported the validity of low temperature processes for single-crystal growth of KTP and concluded that less severe growth parameters could have a dramatic effect on cost and quality of available crystals.[10] To lower the temperature and pressure for hydrothermal growth, an appropriate mineralizer must be chosen. The mineralizer ensures that the KTP solute in the growing zone can reach a supersaturation sufficiently large to grow crystals at a practical rate. Improvements on mineralizers have been reported by Jia et al.[19] and Laudise et al.[13] A novel flux technique described by Ballman et al.[9] utilizes low-viscosity, water-soluble tungstate melts as the solvent. This technique yielded KTP as a single stable phase over its entire cooling range and offered an attractive alternative to complex hydrothermal methods which require high temperatures and pressures.

Jacco has concluded that the future of KTP as a NLO material may indeed depend on solving two recurring problems: crystal size limitations and bulk damage effects.[1] Few papers discuss the problem of residual impurities and thermal history on the properties of KTP crystals. However, some insightful work proposing solutions to these problems does exist and should be noted. Bordui and co-workers[20] have reported the growth of large crystals of KTP through the use of a high-temperature solution and a heat pipe based furnace. The elaborate furnace assembly ensures a high degree of spatial temperature uniformity throughout the

(7) Ouvrard, M. L. *Comptes Rendus* **1890**, *111*, 117.
(8) Jacco, J. C.; Loiacono, G. M.; Jaso, M.; Mizell, G.; Greenberg, B. *J. Cryst. Growth* **1984**, *70*, 484.
(9) Ballman, A. A.; Brown, H.; Olson, D. H.; Rice, C. E. *J. Cryst. Growth* **1986**, *75*, 390.
(10) Belt, R. F.; Gashurov, G. *SPIE Int. Soc. Opt. Eng.* **1988**, *968*, 100.
(11) Laudise, R. A.; Sunder, W. A.; Belt, R. F.; Gashurov, G. *J. Cryst. Growth* **1990**, *102*, 427.
(12) Zumsteg, F. C.; Bierlein, J. D.; Gier, T. E. *J. Appl. Phys.* **1976**, *47*, 4980.
(13) Laudise, R. A.; Cava, R. J.; Caporaso, A. J. *J. Cryst. Growth* **1986**, *74*, 275.
(14) Cai, D.; Yang, Z. *J. Cryst. Growth* **1986**, *79*, 974.
(15) Bolt, R. J. *J. Cryst. Growth* **1993**, *126*, 175.
(16) Bierlein, J. D. US Patent 3,949,323, Apr 1976.
(17) Loiacono, G. M.; McGee, T. F.; Kostecky, G. *J. Cryst. Growth* **1990**, *104*, 389.
(18) Jia, S.; Niu, H.; Tan, J.; Xu, Y.; Tao, Y. *J. Cryst. Growth* **1990**, *99*, 900.
(19) Jia, S.; Jiang, P.; Niu, H.; Li, D.; Fan, X. *J. Cryst. Growth* **1986**, *79*, 970.
(20) Bordui, P. F.; Jacco, J. C.; Loiacono, G. M.; Stolzenberger, R. A.; Zola, J. J. *J. Cryst. Growth* **1987**, *84*, 403.

growth solution. Crystals grown through this technique measured as large as 10 × 10 × 7 mm^3. Uniform and flaw-free growth required controlled dissolution of the original seed surface prior to initiation of supersaturation. It is assumed that this necessity has as its origin a surface degradation phenomenon that occurs during the brief interval the seed crystal is exposed to the air inside the heated furnace prior to its immersion in the growth solution.[20] The importance of this surface degradation phenomena and its relation to high temperature decomposition of $KTiOPO_4$ were discussed by Hagerman et al.[21] and will be examined in more detail in section 3.3.

Growth and characterization of large potassium titanyl phosphate crystals have been completed by Sasaki et al.[22] through the use of a $K_6P_4O_{13}$ flux and a temperature falling method. Strictly controlled cooling rates and a specially designed monitor of crystal weight changes were employed to crystallize KTP as large as 32 × 42 × 87 mm^3. A discussion of the properties of KTP crystals grown from high-temperature tungsten-containing solutions has been reported.[23] The striations observed are detrimental to the optical quality of the crystal and are a result of the incorporation of tungsten during the growth process. This incorporation is a direct result of temperature fluctuations during the growth. A more detailed description of processing–defect–property relationships is provided in section 3. It is important to note that the properties of interest for nonlinear and electrooptical applications are strongly influenced by the choice of growth technique and processing temperature.

1.3. Properties. KTP has been shown to have superior properties for several NLO applications including sum and difference frequency mixing[24-26] and optical parametric oscillation.[27-32] In particular, KTP has been the material of choice for frequency doubling of Nd lasers at 1 μm radiation.[12] Its large electrooptical coefficients coupled with low dielectric constants make it attractive for various electrooptical applications including frequency modulators and Q switches.[6] $KTiOPO_4$ is chemically inert and relatively easy to fabricate.[1] The physical properties of KTP are summarized in Table 1.1. A more detailed list of properties has been provided by Jacco et al.[1] Figure 1.3 provides dispersion curves for KTP.[33] The electrooptical and dielectric properties have been previously reported by Bierlein.[6] Table 1.2 summarizes several of the reported values. Vanherzeele and Bierlein[34] along with Boulanger and co-workers[35] have previously reported the magnitude of the nonlinear optical coefficients of KTP. Table 1.3 summarizes the nonlinear optical and thermal properties of KTP. The d_{ij} values quoted for KTP are given relative to d_{11} of quartz. Dispersion corrections were applied, and the error was ±10%. The large d_{33} coefficient useful for quasi-phase-matched SHG in KTP waveguides validates the observed high conversion efficiency in these structures. The first measurement of d_{eff} by Zumsteg et al.[12] was completed on relatively poor-quality crystals. Since that time several researchers have reported the effective d coefficient for KTP.[36-37] Eckardt and Byer[36] cited a value of 3.2 pm/V. The observed d_{eff} for type II phase matching at 1.064 μm reported by Vanheerzeele and Bierlein,[34] equal to 3.35 pm/V, was in agreement with Eckardt. An alternative calculation method using SHG power with double refraction reported a d_{eff} of 4.3 pm/V.[37]

Table 1.1. Selected KTP Physical Properties (After Jacco et al.[1])

hardness (Knoop)	702
density (g/cm^3)	2.945
thermal conductivity (W/cm K)	0.13
electrical conductivity (c axis, S/cm)	3.5 × 10^{-8} (295 K, 1 kHz)
melting point (°C) (incongruent)	1167
specific heat (cal/g °C)	0.1737

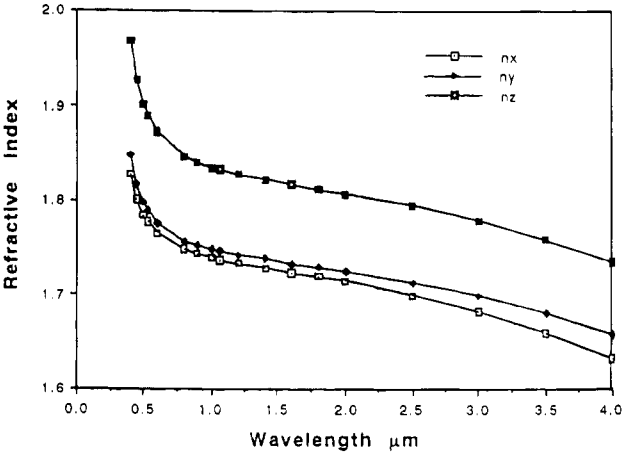

Figure 1.3. Dispersion curves of KTP. (Reprinted with permission from Burnham et al.,[33] copyright 1989 Int. Soc. Opt. Eng.)

Table 1.2. Electrooptic and Dielectric Constants of KTP (After Bierlein[6])

	low freq	high freq
r_{13}	+9.5 pm/V	+8.8 pm/V
r_{23}	+15.7	+13.8
r_{33}	+36.3	+35.0
r_{51}	7.3	6.9
r_{42}	9.3	8.8
r_{c1}	+28.6	+27.0
r_{c2}	+22.2	+21.5
ϵ'_{11}	11.9	11.6
ϵ'_{22}	11.3	11.0
ϵ'_{33}	>17.5	15.4

(21) Hagerman, M. E.; Kozhevnikov, V. L.; Poeppelmeier, K. R. *Chem. Mater.* **1993**, *5*, 1211.
(22) Sasaki, T.; Miyamoto, A.; Yokotani, A.; Nakai, S. *J. Cryst. Growth* **1993**, *128*, 950.
(23) Shumov, D. P.; Tarassov, M. P.; Nikolov, V. S. *J. Cryst. Growth* **1993**, *129*, 635.
(24) Kurokawa, K.; Nakazawa, M. *Appl. Phys. Lett.* **1989**, *55*, 7.
(25) Shen, H. Y.; Zhou, Y. P.; Lin, W. X.; Zheng, Z. D.; Zeng, R. R.; Yu, G. F.; Huang, C. H.; Jiang, A. D.; Jia, S. Q.; Shen, D. Z. *J. Quantum Electron.* **1992**, *28*, 48.
(26) Stolzenberger, R. A. *Photonics Techn. Lett.* **1989**, *1*, 446.
(27) Chung, J.; Siegman, A. E. *J. Opt. Soc. Am. B* **1993**, *10*, 2201.
(28) Kato, K. *J. Quantum Electron.* **1991**, *27*, 1137.
(29) Grasser, C.; Wang, D.; Beigang, R.; Wallenstein, R. *J. Opt. Soc. Am. B* **1993**, *10*, 2218.
(30) Lin, J. T.; Montgomery, J. L. *Opt. Commun.* **1990**, *75*, 315.
(31) Lotshaw, W. T.; Unternahrer, J. R.; Kukla, M. J.; Miyaka, C. I.; Braun, F. D. *J. Opt. Soc. Am. B* **1993**, *10*, 2191.
(32) Wachman, E. S.; Edelstein, D. C.; Tang, C. L. *Opt. Lett.* **1990**, *15*, 136.
(33) Burnham, R.; Dlabal, M. L.; Koechner, W.; Stolzeberger, R.; Pinto, A. *SPIE Int. Soc. Opt. Eng.* **1989**, *1104*, 33.
(34) Vanherzeele, H.; Bierlein, J. D. *Opt. Lett.* **1992**, *17*, 982.
(35) Boulanger, B.; Feve, J. P.; Marnier, G.; Menaert, B.; Cabirol, X.; Villeval, P.; Bonnin, C. *J. Opt. Soc. Am. B* **1994**, *11*, 750.
(36) Eckardt, R.; Byer, R. *SPIE Int. Soc. Opt. Eng.* **1991**, *1561*, 119.
(37) Asaumi, K. *Appl. Phys. B.* **1992**, *54*, 265.

Table 1.3. Nonlinear Optical and Thermal Properties of KTP (After Vanherzeele et al.[34])

property	value
nonlinear optical coefficients (pm/V)	$d_{31} = 6.5$ $d_{32} = 5.0$ $d_{33} = 13.7$ $d_{24} = 7.6$ $d_{15} = 6.1$
temp bandwidth (°C cm)	25
angular bandwidth (mrad cm)[a]	15–68
spectral bandwidth (Å cm)[a]	5.6
Walkoff (mrad)[a]	1
temp coeff of refractive index ($°C^{-1}$)	$\Delta n_x = 1.1 \times 10^{-5}$ $\Delta n_y = 1.3 \times 10^{-5}$ $\Delta n_z = 1.6 \times 10^{-5}$
transmission range (μm)	0.35–4.5
optical absorption (%/cm)	<0.6 (at 1.064 μm) <2 (at 0.532 μm)
thermal expansion coefficients ($°C^{-1}$)	$\alpha_1 = 11 \times 10^{-6}$ $\alpha_2 = 9 \times 10^{-6}$ $\alpha_3 = 0.6 \times 10^{-6}$
thermal conductivity (W/cm °C)	$k_1 = 2.0 \times 10^{-2}$ $k_2 = 3.0 \times 10^{-2}$ $k_3 = 3.3 \times 10^{-2}$
pyroelectric coefficient (nC/cm^2 °C)	7
specific heat (cal/g °C)	0.174

[a] For SHG near 1.0 μm, propagation in the xy plane.

Table 1.4. Properties of Selected Inorganic NLO Crystals (After Eaton[41])

compound	d coefficients[a]	Damage (MW/cm^2) threshold[b]	Cutoff[c]	FOM[d]
β-BaB_2O_4	$d_{11} = 4.1$	10000	198	26
$Ba_2NaNb_5O_{15}$	$d_{31} = 32$	1	370	
KH_2PO_4	$d_{36} = 1$	500	200	1
LiB_3O_5	$d_{32} = 3.1$	2000	165	~1
$LiNbO_3$	$d_{31} = 13$	20	400	
$LiIO_3$	$d_{31} = 10$	50	300	50
$KTiOPO_4$	$d_{31} = 15$	20000	350	215
Urea	$d_{14} = 3$	5000	210	6

[a] Relative to KDP as 1. The d_{36} coefficient is quoted as 0.39 pm/V in ref 95. [b] Damage thresholds are not absolute (experimental conditions can be different). [c] Short-wavelength absorption cutoff in nanometers. [d] The figure of merit, relative to KDP, is a function of the d coefficient, the acceptance angle for phase matchability ($\Delta\theta$), crystal length L, wavelength of input λ, field strength E, and material index of refraction: FOM ~ $(d^2/n^3)(EL/\lambda^2)(\Delta\theta)^2$.

KTP's optical window extends from 0.35 to 4.5 μm.[38] Jacco and Loiacono[39] have reported analyses of the infrared band edge of KTP useful for remote sensing applications. The nonlinear and electrooptical coefficients of KTP along with other important properties compare favorably with other materials for both bulk and waveguide applications. Astill has previously provided a detailed comparison of various figures-of-merit (FOM) for nonlinear optical materials including second harmonic generation.[40] Eaton has also supplied a summary of important properties of selected inorganic NLO crystals (Table 1.4).[41] The angle tuning characteristics of SHG in KTP has been studied by Nishikawa et al.[42] KTP has a waveguide FOM that is twice that of other inorganic materials.[5] The value and significance of the electrooptic waveguide FOM for KTP will be discussed in detail in section 4.

1.4. Applications. Attention has focused on $KTiOPO_4$ for sum and difference frequency mixing, optical parametric oscillation, and electrooptical switching. Its practical value as a nonlinear and electrooptical material results from the following characteristics: (i) large temperature window; (ii) extremely low onset power threshold; (iii) high power conversion efficiency; (iv) wide wavelength range of phase matching capabilities; (v) large nonlinear optical and electrooptical coefficients; (vi) high threshold to laser induced damage.

KTP's unusually large bandwidth makes it advantageous for maintaining the pulsed energy stability of the converted beam.[5] Its low absorption and wide acceptance angle make it a preferred doubling crystal when available peak power is limited. Its insensitivity to piezoelectric and pyroelectric effects coupled with its large temperature and optical window suggest that KTP waveguide devices should have increased thermal and mechanical stability and be able to convert and/or control high-intensity optical beams with input wavelengths ranging from the near ultraviolet to the infrared. According to Bierlein and Vanherzeele,[5] there is an increasing need for design and fabrication of miniature blue and green solid-state laser sources for a variety of applications, including optical scanning, optical data storage, laser printing, and display technology.

Many devices and applications utilize KTP single crystals. KTP crystals have been used as parametric amplifiers for the generation of picosecond tunable infrared radiation.[43] Pump wavelength tuning of optical parametric oscillations and frequency mixing in the KTP-related isomorph, KTA ($KTiOAsO_4$), have been examined by Jani and colleagues.[44] A high-repetition-rate femtosecond optical parametric oscillator based on the KTP isomorph, $RbTiOAsO_4$, has been reported by Powers et al.[45] Sum frequency mixing of red and infrared radiation to generate green light was reported. Nishikawa et al.[46] have demonstrated efficient and tunable parametric superfluorescence in KTP crystals pumped by 1 ps pulses. Picosecond pumped short light pulses have the potential to generate broadly tunable optical pulses from visible to near-IR without using an optical cavity. High-density optical recording using a stable micro green SHG laser consisting of Nd:YVO_4 and KTP has also been achieved.[47] This intracavity green laser has the capability of tripling the storage density of an optical disk owing to higher power conversion and efficiency at lower wavelengths. Noncritically phase-matched (NPM) KTP crystals at room temperature have been systematically analyzed for potential applications in laser tuning of diode-pumped systems.[48,49] A 20 W average-power KTP intracavity-doubled Nd:YAG laser has been developed.[50] Infrared optical parametric oscillation and amplification in KTP has been discussed by

(38) Mangin, J.; Khodjaoui, A.; Marnier, G. *Phys. Status Solidi A* **1990**, *120*, K111.
(39) Jacco, J. C.; Loiacono, G. M. *Appl. Phys. Lett.* **1991**, *58*, 560.
(40) Astill, A. G. *Thin Solid Films* **1991**, *204*, 1.
(41) Eaton, D. F. *Science* **1991**, *253*, 281.
(42) Nishikawa, T.; Uesugi, N.; Ito, H. *Appl. Phys. Lett.* **1989**, *55*, 1943.
(43) Vanherzeele, H. *SPIE Int. Soc. Opt. Eng.* **1989**, *1104*, 44.
(44) Jani, M. G.; Murray, J. T.; Petrin, R. R.; Powell, R.; Loiacono, D. N.; Loiacono, G. M. *Appl. Phys. Lett.* **1992**, *60*, 2327.
(45) Powers, P. E.; Tang, C. L.; Cheng, L. K. *Opt. Lett.* **1994**, *19*, 1439.
(46) Nishikawa, T.; Uesugi, N.; Yumoto, J. *Appl. Phys. Lett.* **1991**, *58*, 1943.
(47) Tatsuno, K.; Takahashi, M.; Muraoka, K.; Sugiyama, H.; Nakamura, J.; Andou, T.; Miyai, T. *Jpn. J. Appl. Phys.* **1992**, *31*, 601.
(48) Lin, J. T. *SPIE Int. Soc. Opt. Eng.* **1989**, *1040*, 129.
(49) Risk, W. P.; Payne, R. N.; Lenth, W.; Harder, C.; Meier, H. *Appl. Phys. Lett.* **1989**, *55*, 1179.
(50) Perkins, P. E.; Fahlen, T. S. *J. Opt. Soc. Am. B.* **1987**, *4*, 1066.

Table 1.5. Properties of 2–4 μm Optical Parametric Converters (After Burnham et al.[33])

material	pump wavelengths (4 μm output), μm	transparency range, μm	figure of merit, M (eq 10)	damage threshold, I_d (MW/cm^2)	pump[a] threshold (MW/cm^2)	I_d/I_t (1 cm crystal)	required crystal length, cm
$AgGaSe_2$	1.5–2.5	0.7–18	40	30	43	0.7	3.7
CdSe	2.5–3.5	0.7–20	24	60	29	2	2.2
KTP	0.5–1.8	0.4–4.2	8	1000	23	40	0.5
$LiIO_3$	0.5–2.4	0.4–5.5	2	100	100	1	3.1
$LiNbO_3$	0.5–2.4	0.5–5.0	4	200	60	3.3	1.7
TAS	1.3–3.0	1.5–20	50	30	6	5	1.4

[a] 1 cm crystal length, 4 μm output.

Burnham et al.[33] and Vanherzeele.[51] Table 1.5 supplies the properties of various optical parametric converters. The use of high-quality KTP crystals and new diode array pumped Nd and other rare-earth solid-state lasers with dramatically increased efficiency have improved the prospects of generating tunable mid-infrared radiation useful for remote sensing applications.[33]

Current development of devices based on KTP single crystals is limited by crystal size, quality, and cost. Both larger and less expensive crystals are needed to promote the use of KTP in the SHG field and to compete with existing $LiNbO_3$ electrooptic modulators. As higher quality crystals of KTP become available at lower costs, it can be increasingly used for sum frequency generation of red, yellow, and blue visible radiation.[1] Optimization of SHG and SFG laser light sources in the visible spectral region requires accurate knowledge of the absolute value of the refractive indexes and the temperature dependence of these values. Wiechman et al.[52] provided refractive index temperature derivatives for KTP. These data may prove crucial in the design of intracavity SHG green light laser sources where variations in KTP retardation can lead to severe output fluctuations. Further discussion of KTP waveguides as laser light sources including integrated optical devices based on single crystal synthesis and thin film fabrication is provided in sections 4 and 6, respectively.

One focus of research in materials chemistry and nonlinear optics has been the study of material properties that modify or mix light waves with optimal transmission and minimal light scattering. The purpose of the NLO material is to introduce strong coupling between the electromagnetic fields of a primary light wave and the secondary field of another source (externally, through an applied field, or internally, through another electromagnetic light wave).[2] Correlations between the microscopic structure of an NLO material and the observed macroscopic property have proven important in the design of new materials and the fabrication of novel photonic devices.

2. Structure–Property Relationships

KTP belongs to a structural family of great diversity and versatility.[53] The vast structure field of potassium titanyl phosphate has inspired numerous studies of the relation between structure and observed nonlinear optic phenomena.[54] The inclusion host–guest relationship and the presence of two formula units in the asymmetric unit with all the available atoms in general positions have made possible a large number of synthetic permutations of the KTP structure.[53] The KTP structure field presents an unusual and unique opportunity to evaluate structure–property relationships at the atomic level and develop a predictive paradigm to create new NLO materials. Stucky et al.[2] have presented detailed studies of the relationship between electrooptic properties, chemical bonding, and small structural displacements within a single topological configuration. The compositional phase space of this field has been approached in terms of the inclusion chemistry of KTP. This approach has proven quite effective in both the development of new NLO materials based on KTP isomorphs and the enhancement of the understanding of bonding relationships which lead to the observed NLO behavior in mixed metal oxides. An understanding of the structure–property relationships in KTP has led to the design of new materials and the fine tuning of single-crystal properties, all of which should prove important in the fabrication and optimization of KTP thin films for photonic device applications.

2.1. $KTiOPO_4$ Structure Field. The KTP structure field has been previously described in detail by Stucky et al.[2] KTP is a member of the family of compounds with the general formula $MM'OXO_4$ where M = K, Rb, Na, Cs, Tl, NH_4, M′ = Ti, Sn, Sb, Zr, Ge, Al, Cr, Fe, V, Nb, Ta, and X = P, As, or Si. Both aliovalent and monovalent substitutions are possible. Choices of M, M′, and X have a dramatic effect on the observed NLO behavior. The guest framework is comprised of potassium ions while the host framework is defined by the extended helical network of TiO_6 octahedra bridged by phosphorus atoms. Modifications can be made to both the host and the guest frameworks by substitution of potassium, titanium, phosphorus, and oxygen. Guest exchange can be completed by substitution during synthesis,[55] ion exchange,[12] or small-molecule gaseous exchange.[56] Specific examples have included:[2] (i) $(M,M')TiOPO_4$ compounds; (ii) $(M,M')TiO(P,As)O_4$ compounds; (iii) tetravalent main-group and transition-metal KTP derivatives; and (iv) mixed-valent KTP isostructures. Table 2.1 lists isomorphic derivatives of KTP along with their second harmonic generation intensities.[2]

In 1989, Stucky et al.[2] concluded that it appeared quite possible that many new NLO materials could be realized through an applied understanding of the multidimensional compositional and structural space available to the KTP family. Consequently, the study and selective tuning of optical properties based on single-crystal synthesis of various isomorphs has been achieved. Since 1989, the structure field of KTP has expanded

(51) Vanherzeele, H. *Appl. Opt.* **1990**, *29*, 2246.
(52) Wiechman, W.; Kubota, S.; Fukui, T.; Masuda, H. *Opt. Lett.* **1993**, *18*, 1208.
(53) Phillips, M. L.; Gier, T. E.; Eddy, M. M.; Keder, N. L.; Stucky, G. D.; Bierlein, J. D. *Solid State Ionics* **1989**, *32/33*, 147.
(54) Cheetham, A. K. *Science* **1994**, *264*, 794.
(55) Phillips, M. L. F.; Harrison, W. T. A.; Gier, T. E.; Stucky, G. D. *SPIE Int. Soc. Opt. Eng.* **1989**, *1104*, 225.
(56) Eddy, M. M.; Gier, T. E.; Keder, N. L.; Stucky, G. D.; Cox, D. E.; Bierlein, J. D.; Jones, G. *Inorg. Chem.* **1988**, *27*, 1856.

Table 2.1. Isomorphous Derivatives of KTP (After Stucky et al.[2])

compound	SHG	a, Å	b, Å	c, Å
(M,M′)$TiOPO_4$ Compounds				
$KTiOPO_4$	6000	12.814	6.404	10.616
$NaTiOPO_4$	160	12.615	6.281	10.585
$AgTiOPO_4$	5	12.524	6.263	10.530
$Ag_{0.85}K_{0.15}TiOPO_4$	7	12.534	6.294	10.524
$Ag_{0.5}K_{0.5}TiOPO_4$	130	12.552	6.333	10.602
$(NH_4)_{0.5}H_{0.5}TiOPO_4$	6	12.822	6.284	10.598
$(NH_4)_{0.5}K_{0.5}TiOPO_4$	1100	12.894	6.442	10.580
$Rb_{0.5}K_{0.5}TiOPO_4$	6000	12.916	6.443	10.546
$TlTiOPO_4$	6000	12.983	6.490	10.578
$(NH_4)_{0.5}(H_3O)_{0.5}TiOPO_4$	700	12.915	6.494	10.589
NH_4TiOPO_4	1100	12.915	6.492	10.598
$RbTiOPO_4$	6000	12.971	6.492	10.577
(M,M′)$TiO(P,As)O_4$ Compounds				
$KTiOAsO_4$	6000	13.103	6.558	10.746
$KTiO(PO_4)_{0.5}(AsO_4)_{0.5}$	6000	12.950	6.478	10.677
$TlTiOAsO_4$	6000	13.208	6.686	10.724
$(NH_4)_{0.5}K_{0.5}TiOAsO_4$	100	13.157	6.592	10.809
$NH_4TiOAsO_4$	100	13.212	6.678	10.793
$RbTiOAsO_4$	6000	13.242	6.689	10.755
$Cs_{0.5}K_{0.5}TiOAsO_4$	6700	13.311	6.662	10.800
Tetravalent Main-Group and Transition-Metal KTP Derivatives				
$NaGeOPO_4$	4	12.326	6.094	10.117
$KGeOPO_4$	3.3	12.602	6.302	10.006
$KVOPO_4$		12.717	6.382	10.513
$KGeOAsO_4$	0.3	12.85	6.54	10.08
$KSnOPO_4$	0.0	13.146	6.528	10.727
$RbSnOPO_4$	0.0	13.332	6.618	10.720
$KSnOAsO_4$	0.53	13.417	6.687	10.977
$RbZrOAsO_4$	3	13.735	6.908	11.440
$NH_4ZrOAsO_4$	1	13.681	6.886	11.583
$CsZrOAsO_4$	2	13.796	6.982	11.23
Mixed-Valent KTP Isostructures				
$KGaPO_4F_{0.7}(OH)_{0.3}$	0.72	12.715	6.304	10.433
$KTi_{0.5}Ga_{0.5}O_{0.5}PO_4F_{0.35}(OH)_{0.15}$	200	12.802	6.352	10.503
$KFePO_4F$	2.66	12.854	6.372	10.670
$KGa_{0.5}Nb_{0.5}OPO_4$	1.0	12.94	6.47	10.62
$RbGa_{0.5}Nb_{0.5}OPO_4$	1.0	13.107	6.490	10.490
$KFe_{0.5}Nb_{0.5}OPO_4$	2.7	12.960	6.466	10.696
$KGaAsO_4F$	0.02	13.04	6.47	10.61
$KMg_{0.33}Nb_{0.67}OPO_4$	0.0	13.079	6.516	10.929
$KMn_{0.5}Nb_{0.5}OPO_4$	0.0	13.122	6.569	10.911
$KGa_{0.5}Nb_{0.5}OAsO_4$	1.0	13.24	6.62	10.8
$KFeAsO_4F$	1.0	13.21	6.54	11.15
$KGa_{0.5}Nb_{0.5}OAsO_4$	5.5	13.403	6.71	10.74

from over 40 members to nearly 100; these new isomorphs and KTP related phases are summarized in Table 2.2.[57-69] Note that unlike Table 2.1, the SHG intensities are normalized with respect to that of $KTiOPO_4$ which is taken as unity. This structure field continues to expand and while not all new isomorphs are provided an attempt has been made to provide a sampling of each class of derivatives.

Table 2.2. New Isomorphous Derivatives of KTP

compound	SHG	a, Å	b, Å	c, Å	ref
(M,M′)$TiOPO_4$ Compounds					
$KTiOPO_4$	1.00	12.823(4)	6.416(6)	10.589(3)	57
$Na_{0.95}K_{0.05}TiOPO_4$	0.11	12.611(2)	6.281(1)	10.595(2)	57
$Ag_{0.85}K_{0.15}TiOPO_4$	0.01	12.534(2)	6.294(1)	10.524(2)	57
$K_{0.55}Li_{0.45}TiOPO_4$	0.68	12.778(2)	6.370(1)	10.560(1)	57
$K_{0.5}Rb_{0.5}TiOPO_4$		12.8961(1)	6.4299(5)	10.5929(8)	58
$K_{0.5}Na_{0.5}TiOPO_4$		12.75613(7)	6.3189(4)	10.60426(6)	59
$K_{0.42}Na_{0.58}TiOPO_4$		12.7298(2)	6.3074(4)	10.6073(1)	60
$Rb_{0.5}Na_{0.5}TiOPO_4$		12.8273(6)	6.3347(3)	10.6052(5)	59
(M,M′)$TiO(P,As)O_4$ Compounds					
$KTiOAsO_4$	1.09	13.416(5)	6.584(2)	10.771(6)	57
$Na_{0.87}K_{0.13}TiOAsO_4$	0.87	12.888(1)	6.4095(1)	10.7393(6)	57
$Na_{0.98}K_{0.02}TiOAsO_4$	0.01	12.792(3)	6.422(2)	10.683(4)	57
$K_{0.54}Li_{0.46}TiOAsO_4$	1.07	13.059(9)	6.588(6)	10.734(8)	57
$Rb_{0.91}Cs_{0.09}TiOAsO_4$					61
$Cs_{0.84}K_{0.16}TiOAsO_4$					61
$KTiO(P_{0.5}As_{0.5})O_4$		12.9695(8)	6.4932(4)	10.6898(7)	62
$KTiO(P_{0.76}As_{0.24})O_4$					63
Tetravalent Main-Group and Transition-Metal KTP Derivatives					
$KTiSnOPO_4$		13.129(3)	6.518(3)	10.708(4)	64
$KTi_{0.9}Sn_{0.1}OPO_4$		12.844(1)	6.420(1)	10.591(1)	64
$KTi_{0.67}Sn_{0.33}OPO_4$		12.906(2)	6.468(3)	10.618(2)	64
$KTi_{0.5}Sn_{0.5}OPO_4$		12.929(4)	6.447(3)	10.626(2)	64
$KTi_{0.5}Sn_{0.5}OPO_4$		12.9764(3)	6.4669(1)	10.6461(2)	65
$K_{0.5}Rb_{0.5}SnOPO_4$		13.2382(4)	6.5581(2)	10.7083(3)	66
$K_{0.5}Na_{0.5}Ti_{0.5}Sn_{0.5}OPO_4$		12.8826(4)	6.3898(2)	10.6384(4)	66
$Na_{0.5}Rb_{0.5}Ti_{0.5}Sn_{0.5}OPO_4$		13.1435(5)	6.5478(3)	10.6433(3)	66
$K_{0.5}Rb_{0.5}Ti_{0.5}Sn_{0.5}OPO_4$		13.0440(5)	6.4961(3)	10.6304(4)	66
Mixed-Valent KTP Isostructures					
$KNb_{0.5}Ti_{0.5}OPO_4$		12.976(5)	6.488(4)	10.773(7)	67
$KNb_{0.5}V_{0.5}OPO_4$		12.949(6)	6.431(8)	10.686(4)	67
$KNb_{0.5}Cr_{0.5}OPO_4$		12.894(7)	6.435(6)	10.629(6)	67
$KNb_{0.5}Fe_{0.5}OPO_4$		12.956(9)	6.467(5)	10.698(8)	67
$KTa_{0.5}Ti_{0.5}OPO_4$		12.981(8)	6.484(7)	10.763(8)	67
$KTa_{0.5}V_{0.5}OPO_4$		12.985(4)	6.442(3)	10.696(4)	67
$KTa_{0.5}Cr_{0.5}OPO_4$		12.914(5)	6.433(3)	10.670(6)	67
$KTa_{0.5}Fe_{0.5}OPO_4$		13.045(7)	6.450(8)	10.662(6)	67
$K_{0.5}Nb_{0.5}Ti_{0.5}OPO_4$	0.90	12.879(9)	6.402(7)	10.659(4)	67
$K_{0.5}Nb_{0.5}V_{0.5}OPO_4$	0.50	12.801(6)	6.357(4)	10.569(4)	67
$K_{0.5}Ta_{0.5}Ti_{0.5}OPO_4$	0.80	12.852(9)	6.409(8)	10.663(6)	67
$K_{0.5}Ta_{0.5}V_{0.5}OPO_4$	0.40	12.819(7)	6.367(4)	10.615(5)	67
$KTi_{0.85}V_{0.15}OPO_4$	0.10	12.808(5)	6.400(6)	10.578(6)	67
$K_{0.85}Ti_{0.85}V_{0.15}OPO_4$	0.36	12.800(6)	6.364(3)	10.572(8)	67
$KTi_{0.75}V_{0.25}OPO_4$	0.05	12.812(6)	6.401(6)	10.569(8)	67
$K_{0.75}Ti_{0.75}V_{0.25}OPO_4$	0.24	12.723(8)	6.340(5)	10.561(8)	67
$KTi_{0.50}V_{0.50}OPO_4$		12.799(7)	6.390(6)	10.560(4)	67
$K_{0.67}Ti_{0.50}V_{0.50}OPO_4$	0.20	12.716(4)	6.363(3)	10.529(5)	67
$K_{0.84}Nb_{0.08}Ti_{0.92}OPO_4$		12.815(4)	6.413(2)	10.597(3)	68
$K_{0.88}Nb_{0.12}Ti_{0.88}OPO_4$		12.809(3)	6.416(2)	10.590(7)	69

The effects of substitution chemistry in the KTP structure field have been extensively examined by Phillips et al.[70] The substitution of monovalent cations larger than K^+ such as Rb^+, NH_4^+, and Tl^+, resulted in little to no change in NLO susceptibility while smaller cation substitutions (Na^+, Ag^+, Li^+) had extremely deleterious effects on the NLO properties.[57] Phillips and co-workers[70] have noted that the variance in NLO susceptibilities among KTP isostructures could be caused not only by changes in the Ti–O bond distances but also by changes in the relative orientations of the TiO_6 octahedra. It was shown that the observed SHG intensities of KTP and related isomorphs were correlated with the average distance between the guest cations and the titanyl oxygen atoms that link adjacent TiO_6 octahedra (Figure 2.1).[57] Phillips et al. concluded

(57) Phillips, M. L. F.; Harrison, W. T. A.; Stucky, G. D. *SPIE Int. Soc. Opt. Eng.* **1991**, *1561*, 84.
(58) Crennell, S. J.; Owen, J. J.; Greg, C. P.; Cheetham, A. K.; Kaduk, J. A.; Jarman, R. H. *J. Mater. Chem.* **1991**, *1*, 113.
(59) Crennell, S. J.; Cheetham, A. K.; Kaduk, J. A.; Jarman, R. H. *J. Mater. Chem.* **1991**, *1*, 297.
(60) Crennell, S. J.; Morris, R. E.; Cheetham, A. K.; Jarman, R. H. *Chem. Mater.* **1992**, *4*, 82.
(61) Mangin, J.; Marnier, G.; Boulanger, B.; Menaert, B. *Inst. Phys. Conf. Ser.* **1989**, *103 (I)*, 65.
(62) Crennel, S. J.; Cheetham, A. K.; Jarman, R. H.; Thrash, R. J.; Kaduk, J. A. *J. Mater. Chem.* **1992**, *2*, 383.
(63) Cheng, L. K.; Bierlein, J. D.; Ballman, A. A. *Appl. Phys. Lett.* **1991**, *58*, 1937.
(64) Jarman, R. H.; Grubb, S. G. *SPIE Int. Soc. Opt. Eng.* **1988**, *968*, 108.
(65) Crennell, S. J.; Owen, J. J.; Cheetham, A. K.; Kaduk, J. A.; Jarman, R. H. *Eur. J. Solid State Inorg. Chem.* **1991**, *t28*, 397.
(66) Crennell, S. J.; Cheetham, A. K.; Kaduk, J. A.; Jarman, R. H. *J. Mater. Chem.* **1992**, *2*, 785.
(67) Gopalakrishnan, J.; Rangan, K. K.; Prasad, B. R.; Subramanian, C. K. *J. Solid State Chem.* **1994**, *111*, 41.
(68) Thomas, P. A.; Watts, B. E. *Solid State Commun.* **1990**, *73*, 97.
(69) Cheng, L. T.; Cheng, R. L.; Harlow, R. L.; Bierlein, J. D. *Appl. Phys. Lett.* **1994**, *64 (2)*, 155.

(70) Phillips, M. L. F.; Harrison, W. T. A.; Stucky, G. D.; McCarron, E. M., III.; Calabrese, J. C.; Gier, T. E. *Chem. Mater.* **1992**, *4*, 222.

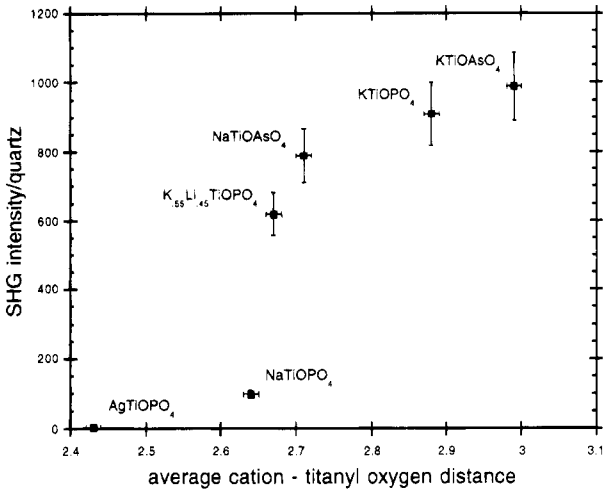

Figure 2.1. Plot of SHG intensity vs average cation-titanyl oxygen bond distance in KTP isostructures. (Data reported in Phillips et al.;[57] figure courtesy of author.)

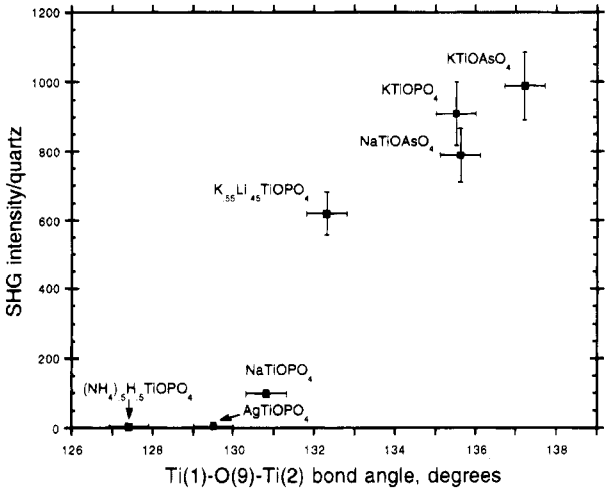

Figure 2.2. Optical nonlinearity and titanyl chain agle in ion-exchanged KTP and KTA derivatives. (Data reported in Phillips et al.;[57] figure courtesy of author.)

that a shorter average distance decreased the charge-transfer excited-state character mixing thus reducing the hyperpolarizability and attenuating the macroscopic nonlinear susceptibility. Figure 2.2 provides further evidence of the influence of octahedral distortion and titanyl chain angle (Ti(1)−O(9)−Ti(2)) on the optical nonlinearity in the KTP structure field.[57] As the titanyl chain angle in KTP isomorphs increased, a corresponding increase in NLO response was observed. The substitution of late-first-row and second-row transition metals and main-group elements for Ti yielded structures similar to KTP. However, the TiO_6 distortion in many cases was not conserved, and a resultant decrease in optical nonlinearity was observed (Figure 2.3). Phillips et al.[70] concluded that the lack of distortion was a result of the absence of low-lying empty d orbitals which reduces the mixing coefficients responsible for the magnitude of the octahedral distortion and the amount of charge transfer in the bonding orbitals. Section 2.2 provides a more detailed account of KTP's complex NLO behavior.

We can now examine specific examples of isomorphous substitution in the KTP structure field which provide further evidence of the relationships between octahedral distortion, optical nonlinearity, and cation

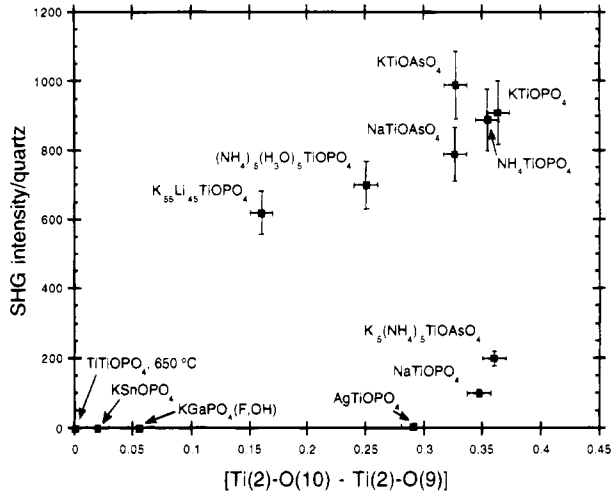

Figure 2.3. Plot of SHG intensity vs $Ti(2)O_6$ distortion in the KTP structure field. (Data reported in Phillips et al.;[57] figure courtesy of author.)

ordering. The effects of cation exchange on the structure of KTP are complex and manyfold. It has been observed that cation ordering may be a common feature of solid solutions of KTP isomorphs.[65] Isomorphous substitution and structural characterization of $K_{0.5}Na_{0.5}TiOPO_4$ and $K_{0.5}Rb_{0.5}TiOPO_4$, an isomorph of particular interest for waveguide technology, have been completed.[58] Complete ordering of Na on the K(1) site in $K_{0.5}Na_{0.5}TiOPO_4$ and Rb on the K(2) site in $K_{0.5}Rb_{0.5}TiOPO_4$ were demonstrated by both neutron diffraction and NMR spectroscopy. Crennell et al.[60] have proposed that the main role of the cation may be to modify the degree of delocalization along the Ti−O chain through its interaction with O(9) and subsequent effect on the Ti(1)−O(9)−Ti(2) bond angle.

In an attempt to further understand the role of various transition-metal ions on the NLO properties of the KTP family, Thomas and Watts[68] have reported Nb doping on the Ti(1) site. Gopalakrishnan et al.[67] have synthesized and investigated a number of aliovalent KTP analogues of the general formula $KM_{0.5}M'_{0.5}PO_4$ ($M = Nb^{5+}$, Ta^{5+}; $M' = Ti^{3+}$, V^{3+}, Cr^{3+}, Fe^{3+}). The authors also synthesized new Ti^{4+} and V^{4+} derivatives, $K_{0.5}M_{0.5}M'_{0.5}OPO_4$ ($M = Nb^{5+}$, Ta^{5+}; $M' = Ti^{4+}$, V^{4+}). Substitution of as much as 50% of the pentavalent Nb and Ta for Ti does not destroy the SHG behavior. Their work is in agreement with Phillips' conclusion that substitution of d^0 cations such as Nb^{5+} and Ta^{5+} which support the ferroelectric distortion of metal−oxygen octahedra does not adversely affect the SHG property of KTP. All other substitutions of transition-metal ions (Ti^{3+}, V^{3+}, Cr^{3+}, Fe^{3+}) that absorb in the visible and do not support a ferroelectric distortion of the anionic groups destroy the NLO property.

The substitution of As for P has gained particular interest since Bierlein et al.[6] discovered that $KTiOAsO_4$ (KTA) had significantly improved NLO properties. Compared to KTP, KTA has a higher figure-of-merit for SHG, larger electrooptic coefficients, and lower ionic conductivity. The origin of an enhanced NLO response for KTA remains unclear and continues to be the subject of further investigations.[71] Crennell et al.[62] have re-

(71) Cheng, L. T.; Cheng, L. K.; Bierlein, J. D.; Zumsteg, F. C. *Appl. Phys. Lett.* **1994**, *63*, 2618.

ported the structure of $KTiO(P_{0.5}As_{0.5})O_4$ (KTAP). Powder SHG measurements revealed a correlation between the Ti(1)–O(9)–Ti(2) bond angle and the NLO coefficients in the KTAP system. The occupancy of the P sites was essentially random unlike the clear ordering seen on partial substitution for K or Ti. However, the bond angles in the titanyl chain continued to increase as P was replaced with As. Optically clear crystals of KTA isomorphs with the general formula $Cs_xM_{1-x}TiOAsO_4$ where (M = K, Rb) also showed increased nonlinear susceptibilities.[61] The transparency range and ferroelectric phase transition temperature were studied and correlated with the observed structure; see section 2.3. Crosnier et al.[72] have reported another interesting KTP isostructure, $KSbOSiO_4$. The framework structure is isotypic with that of KTP and built up from SiO_4 tetrahedra and SbO_6 octahedra.

Bulk KTP is not suitable for NLO applications at high optical frequencies owing to the loss of phase matching capability at wavelengths shorter than 990 nm and absorption in the near ultraviolet. Because of the increased interest in manufacturing compact diode-pumped solid-state lasers with wavelengths in the visible region, emphasis on expanding the phase-matching capability of KTP through isomorphous substitution has been examined. Phillips et al.[55] have previously described the search of the $MM'OPO_4$ structure field for materials with enhanced NLO response and phase-match conditions outside of typical frequency limits. It was proposed that replacing the d^0 Ti^{4+} ions with main-group metal ions would enhance UV transparency and potentially alter refractive indexes and thus their phase matching properties. Jarman et al.[64] have described the growth of a series of crystals with enhanced UV transparency, $KTi_{1-x}Sn_xOPO_4$, from high-temperature solution, and the characterization of optical properties using standard powder techniques. The magnitude of SHG obtained from a 1.06 μm pump laser decreased with increasing x to near zero at $x = 1$. The structure of KSP ($x = 1$) was very close to the centrosymmetric structure which has been identified[64] as the likely high-temperature prototype structure for materials in the KTP family (section 2.3). The solid solution KTP isomorphs, $K_{1-x}Nb_xTi_{1-x}OPO_4$ and $K_{1-x}Ta_xTi_{1-x}OPO_4$, suitable for SHG of blue light have been reported by Cheng et al.[69] The observed nonlinear susceptibilities were found to depend on Nb doping levels with an optimal phase matching for $x = 0.12$. Site selective substitution of Nb for Ti(1) was observed. This extension to the blue spectral region makes KTP useful for optical data storage and medical diagnostics.

In a waveguide configuration, structurally induced birefringence (the difference in effective index between TE-like and TM-like modes) may provide an alternative way to achieve phase matching at shorter wavelengths.[73] The optical birefringence of KTP has been examined by Pisarev et al.[74] and Shaldin et al.[75] Quasi-phase-matching through periodic reversal of the polar axis is also more easily effected in a waveguide configuration and will be discussed in section 4. The temperature dependence of polarization reversal is important for waveguide processing parameters and has been studied by Mangin and co-workers.[76]

The structure field of KTP continues to expand along with the tuning of desired NLO properties through exhaustive isomorphous substitutions. In the following section we will examine work on the development of a phenomenological theory to explain the NLO behavior of all existing isostructures.

2.2. Theory of Nonlinear Optical Behavior. Zumsteg et al.[12] first introduced KTP as an NLO material in 1976 and reported the results of using Levine's bond charge model[77] to calculate the microscopic susceptibilities in the $K_{1-x}Rb_xTiOPO_4$ system. They concluded that the short Ti–O bond lengths in the $[TiO_6]^{8-}$ anionic groups were the principal contributors to the SHG tensor, d_{ijk}. The results of Hansen et al.[78] were in agreement with the conclusions of Zumsteg et al.[12] and Levine.[77] However, both models gave calculated values of SHG coefficients that were substantially lower than the observed experimental values. Chen's anionic group model assigns the distortion of the Ti coordination sphere as the major contributor to d_{ijk} in KTP.[79] This model provides a more extended treatment of the electronic hyperpolarizability which is defined within the anionic cluster, $[TiO_6]^{8-}$, by the degree of mixing between molecular orbitals with varying distributions of electron density.

In ferroelectric mixed metal oxides such as KTP, the metal coordination sphere distorts via a second-order Jahn–Teller effect.[80] This distortion stabilizes the bonding (occupied) orbitals, which have oxygen character, at the expense of the antibonding (empty) orbitals, which have metallic character. Comparisons have been drawn between the long–short metal oxygen bonds in the KTP Ti–O chain (also present in other ferroelectric metal oxides) and the alternating single and double bonds of conjugated π systems in organic compounds.[57] More specifically, Phillips et al.[81] have postulated that this conjugation results in a delocalized excited state in which unoccupied higher energy orbitals of metallic character overlap to form a charge-transfer band. The distortion of the titanium anionic octahedra allows the dipolar excited states to mix with the bonding electronic states thus imparting a strong hyperpolarizability to the titanyl chain.

It has been clear from structural studies on the compounds in the KTP field that earlier structure–property models do not predict the observed SHG response. Inclusion tuning experiments have indicated that it is not possible to treat the host framework independently of the cations and arrive at a reasonable model for all compounds.[2] Munowitz et al.[82–84] have provided systematic theoretical studies of the nonlinear

(72) Crosnier, M.; Guyomard, D.; Verbaere, A.; Piffard, Y. *Eur. J. Solid State Inorg. Chem.* **1990**, *t27*, 845.
(73) Wood, V. E., personal correspondence.
(74) Pisarev, R. V.; Kizhaer, S. A.; Jamet, J. P.; Ferre, J. *Solid State Commun.* **1989**, *72*, 155.
(75) Shaldin, Y. V.; Poprawski, R. *J. Phys. Chem. Sol.* **1990**, *51*, 101.
(76) Mangin, J.; Jeandel, G.; Marnier, G. *Phys. Status Solidi A* **1990**, *117*, 319.
(77) Levine, B. F. *Phys. Rev. B.* **1973**, *7*, 2600.
(78) Hansen, N. K.; Protas, J.; Marnier, G. *C. R. Acad. Sci. Paris Ser. II* **1988**, *307*, 475.
(79) Chen, C. T. *Annu. Rev. Mater. Sci.* **1986**, *16*, 203.
(80) Burdett, J. K.; Hughbanks, T. *Inorg. Chem.* **1985**, *24*, 1741.
(81) Phillips, M. L. F.; Harrison, W. T. A.; Gier, T. E.; Stucky, G. D.; Kulkarni, G. V.; Burdett, J. K. *Inorg. Chem.* **1990**, *29*, 2158.
(82) Munowitz, M.; Jarman, R. H.; Harrison, J. F. *Chem. Mater.* **1992**, *4*, 1296.
(83) Munowitz, M.; Jarman, R. H.; Harrison, J. F. *J. Phys. Chem.* **1992**, *96*, 124.

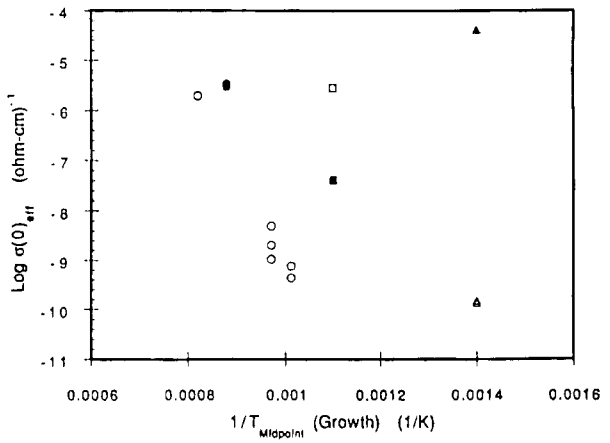

Figure 2.4. Room Temperature ionic conductivity of KTP plotted as a function of the reciprocal midpoint growth temperature: flux 1 (○), flux 2 (●), high-temperature hydrothermal A (■) and B (□), low-temperature hydrothermal (△), and Ba ion-exchanged low-temperature hydrothermal (▲). (Reprinted with permission from Morris et al.,[87] copyright 1991 Int. Soc. Opt. Eng.)

optical properties of KTP. A primary goal of their studies has been the understanding of the relationship between microscopic structure and macroscopic properties. A series of models to investigate the influence of host and guest frameworks on the large second-order susceptibilities of KTP were evaluated through the standard quantum mechanics sum-over-states approach. Their conclusions were in agreement with those of Stucky and Phillips.[2] That is, molecular orbital pictures developed from isolated fragments may be insufficient to accurately model the cooperative nonlinear response of highly delocalized systems such as KTP.[84] Work continues on the development of a comprehensive theory which accurately models the influence of the microscopic structure of KTP on the observed macroscopic properties such as ionic conductivity, ferroelectricity and high temperature structural changes.

2.3. Ionic Conductivity, Ferroelectricity, and High-Temperature Structural Changes. Specific characteristics of the complex structure of KTP have been examined to explain the observed ionic conductivity, ferroelectricity, and high-temperature structural changes. A practical understanding of these characteristics is essential in the preparation and applications of KTP and related isomorphs. KTP is known as a quasi-one-dimensional superionic conductor of K^+ ions.[85] The ionic conductivity along the *c* axis is greater by 4 orders of magnitude than that perpendicular to the *c* axis.[86] As a result, the K^+ ions are considered to move preferentially along the channels parallel to the polar or *c* axis. The magnitude of the AC conductivity of KTP also varies substantially depending on the technique and conditions of growth (Figure 2.4).[87] The anisotropic behavior of the ionic conductivity of KTP has been explained through careful consideration of the conduction paths of the potassium ions and the size of the bottlenecks deduced from the crystal structure.[88] Nonstoichiometric composition or other unknown K^+ ion sites may exist in these channels. Bierlein and Vanherzeele[5] have proposed that the mechanism of ion conduction in KTP is a potassium vacancy mechanism. Consequently, a direct relation has been observed between ionic conductivity and the content of trivalent cations such as Al^{3+}, V^{3+}, Ga^{3+}, and Cr^{3+}.[10] Trivalent cation doping reduces the ionic conductivity parallel to the 2-fold axis of KTP and thus alters the physical properties of the material. Chromium exhibits a strong preferential incorporation in KTP. In contrast, it has also been shown that the conductivity and low-frequency dielectric constant of KTP can be significantly enhanced by partial substitution of Nb^{5+} for Ti^{4+} while substitution of Zr^{4+} and Sn^{4+} for Ti^{4+} does not alter these properties.[89] It was concluded that the observed enhancement of conductivity in Nb-substituted KTP was a result of the creation of vacancies at the K sites.

Crystals of KTP, RTP, and TlTP were grown, studied, and found to be ferroelectrics with Curie points of 934, 789, and 581 °C, respectively.[90] The examination of physical properties indicated that at low temperatures, the crystals were polar and belonged to the acentric crystal class, *mm*2. Owing to the high conductivity of these compounds, it was impossible to observe the dielectric hysteresis loops and determine the magnitude of their spontaneous polarization. Yanovskii et al.[90] concluded that the ferroelectric phase transitions were apparently responsible for the large NLO susceptibility coefficients of KTP whereas the high mobility of potassium cations provided explanation of the high threshold to laser-induced damage. They concluded that the compounds underwent phase transitions at the Curie point described by the change in symmetry ($Pna2_1$(noncentrosymmetric) → *Pnam*(centrosymmetric)). Recent studies of high-temperature structural changes in KTP and related isomorphs have indicated that the proper assignment for the change in symmetry is actually ($Pna2_1 \rightarrow Pnan$).[91-95] At the Curie point, KTP undergoes a phase transition to a centrosymmetric space group in which both K sites become equivalent. The distortion of the Ti octahedra and resultant NLO response decrease with increasing temperature. Similar effects have been observed in other ferroelectric mixed metal oxides. Gallagher et al.[96] have examined the effects of TiO_2 addition to $LiNbO_3$ on cation vacancy content, Curie temperature, and changes in lattice constants. Structural changes at the Curie temperature have been correlated to existing defect models. Similar

(84) Munowitz, M.; Jarman, R. H.; Harrison, J. F. *Chem. Mater.* **1993**, *5*, 661.
(85) Bierlein, J. D.; Arweiler, C. B. *Appl. Phys. Lett.* **1986**, *49*, 917.
(86) Morris, P. A.; Ferretti, A.; Bierlein, J. D. *J. Cryst. Growth* **1991**, *109*, 367.
(87) Morris, P. A.; Crawford, M. K.; Roelofs, M. G.; Bierlein, J. D.; Baer, T. M. *SPIE Int. Soc. Opt. Eng.* **1991**, *1561*, 104.
(88) Furusawa, S.; Hayasi, H.; Ishibashi, Y.; Miyamoto, A.; Sasaki, T. *J. Phys. Soc. Jpn.* **1993**, *62*, 183.
(89) Sastry, P. U. M.; Somayazulu, M. S.; Sequiera, A. *Mater. Res. Bull.* **1992**, *27*, 1385.
(90) Yanovsii, V. K.; Voronkova, V. I. *Phys. Status Solidi A* **1980**, *93*, 665.
(91) Harrison, W. T. A.; Gier, T. E.; Stucky, G. D.; Schultz, A. J. *J. Chem. Soc., Chem. Commun.* **1990**, 540.
(92) Thomas, P. A.; Glazer, A. M.; Watts, B. E. *Acta. Crystallogr., Sect. B* **1990**, *46*, 333.
(93) Godfrey, K. W.; Thomas, P. A.; Watts, B. E. *Mater. Sci. Eng.* **1991**, *9*, 479.
(94) Thomas, P. A.; Mayo, S. C.; Watts, B. E. *Acta. Crystallogr., Sect. B* **1992**, *48*, 401.
(95) Northrup, P. A.; Parise, J. B.; Cheng, L. K.; Cheng, L. T.; McCarron, E. M., III *Chem. Mater.* **1994**, *6*, 434.
(96) Gallagher, P. K.; O'Bryan, H. M. *J. Am. Ceram. Soc.* **1988**, *71*, C56.

Table 3.1. Defect Chemistry of NLO Mixed Metal Oxides (After Morris et al.[97])

crystal	nonstoichiometry[a]	defects[b]
$BaTiO_3$	$Ba_{(1-x)}TiO_{(3-x)}$, $x \cong 0.01$	V_{Ba}'', $V_O^{\bullet\bullet}$
$LiNbO_3$	$Li_{(1-x)}NbO_3$, $x = 0.036$	$Nb_{Li}^{\bullet\bullet\bullet\bullet}$, V_{Nb}'''''
$Sr_{(1-x)}Ba_xNb_2O_6$	$Sr_{(1-x)}Ba_xNb_2O_6$, $x = 0.39$	
$Ba_2NaNb_5O_{15}$	$Ba_2Na_{0.72}Nb_5O_{15}$	V_{Na}'
$K_3Li_2Nb_5O_{15}$	$K_{2.786}Li_{1.989}Nb_5O_{15}$	V_K', V_{Li}'
$KTiOPO_4$	$K_{(1-x)}TiPO_{(5-x/2)}$, $x \cong 0.0005$[c]	V_K', $V_O^{\bullet\bullet}$
$KTiOAsO_4$[d]		V_K', $V_O^{\bullet\bullet}$, $\{As_{Ti}'\}$[e]
β-Ba_2BO_4[d]		$\{V_{Ba}''\}$,[e] $\{V_O^{\bullet\bullet}\}$[e]
LiB_3O_5[d]		$\{V_{Li}'\}$,[e] $\{V_O^{\bullet\bullet}\}$[e]

[a] Representative of the range of intrinsic nonstoichiometry in as-grown crystals. [b] The defects are presented as being fully ionized. [c] Represents typical flux grown crystals. [d] Defect structure in crystals presently grown are thought to be extrinsically controlled. [e] These defects are suspected; insufficient data exists for confirmation.

correlations are being investigated in the KTP structure field.

We have noted the influence of the structure of KTP on specific properties of interest for nonlinear and electrooptical applications. In section 3, we will examine the correlation between the structure of KTP and the complex defect chemistry of this remarkable photonic material.

3. Processing–Defect–Property Relationships

The properties of NLO materials such as KTP are often determined by the defect structures introduced by the processing procedures used to produce bulk crystals, thin films, and waveguide devices. Morris has provided a summary of the status of crystalline nonlinear optical oxides with respect to the known defects and properties of interest for device applications.[3] Morris described the processing–defect–property relationships for the following NLO mixed metal oxides: $LiNbO_3$, $BaTiO_3$, $KTiOPO_4$, $KTiOAsO_4$, β-BaB_2O_4, and LiB_3O_5. Specifically, the review focused on the defects and properties of NLO oxides produced as a result of bulk crystal growth, post-processing procedures (annealing and waveguide fabrication), and thin-film fabrication. An important conclusion drawn by Morris was that there was insufficient information concerning the defects and properties of NLO mixed-metal oxide thin films. Because thin films are attractive for future integrated optical applications, techniques to produce thin films of KTP are currently being developed along with detailed studies of film properties and defect structures; see section 5. The basic structural units responsible for second-order nonlinear optical susceptibility in most oxide crystals are the acentric anionic groups ($[TiO_6]^{8-}$ for KTP).[3] Defects which modify the bonding of these groups can have a dramatic effect on the observed NLO behavior of these materials. Table 3.1 presents the relevant defect chemistry of important NLO mixed-metal oxides.[97] Careful consideration of the processing–defect–property relationships of KTP has proven essential in the development of devices based on KTP single crystals and will undoubtably prove vital in the development of photonic devices based on thin-film fabrication.

(97) Morris, P. A. *Materials for Nonlinear Optics: Chemical Perspectives*; Marder, S. R., Sohn, J. E., Stucky, G. D., Eds.; ACS Symposium Series No. 445; American Chemical Society: Washington, DC, 1991; p 380.

3.1. Defect Chemistry. KTP has a complex high-temperature defect chemistry which produces a marked effect on the observed nonlinear and electrooptical behavior. As a result, the optimal technique for growing KTP crystals is not clear.[3] Crystal properties vary based on the specific growth technique and processing temperature used. Importantly, low-temperature hydrothermal growth has led to superior crystals with respect to optical damage susceptibility.[98] While the reported linear, nonlinear, and electrooptical coefficients of crystals grown by both flux and hydrothermal techniques are remarkably similar, important properties for device applications, namely, ionic conductivity and damage susceptibility, depend on the specific growth technique used.[5] The ionic conductivity is extremely important in the current processing of KTP single-crystal waveguides and strongly influences device stability.[99]

The anisotropic ionic conductivity can be correlated to the complex defect chemistry of KTP. At temperatures near 900 °C, KTP undergoes the following defect formation reaction:[99]

$$KTiOPO_4(s) \rightarrow K_{1-x}TiOPO_{4(1-x/8)}(s) + (x/2)K_2O(g)$$

where x is the concentration of potassium vacancies. Potassium plays a crucial role in the stability of the KTP structure, and existing defect mechanisms involve potassium vacancies.[5] The presence of nonstoichiometry on the K and O sublattices which increases in magnitude with temperature has been proposed.[87] The predominant defects compensating for the formation of $V_{K's}$ in flux and hydrothermal materials are $V_{O's}$ and OH^-, respectively.[99]

The K^+ ions occupy two positions relative to the 2_1 screw axis (c axis or [001]). Channels parallel to the c axis provide the one-dimensional conductor path for K^+. There are ten inequivalent oxygen sites per unit cell (eight Ti–O–P bonds and two Ti–O–Ti bonds); each of which can presumably be protonated.[99] Ti–(OH)–Ti bonds seem more likely and have been reported.[56] Variations in the concentrations and distributions of the OH^- defects have been measured by infrared spectroscopy (Figure 3.1).[100] The variations observed were attributed to differences in growth environments and other non-hydrogenic defects present in the crystals. The temperature dependence of the peak frequencies and widths measured were consistent with the presence of mobile protons in the lattice. Protons present in the lattice are believed to contribute to the high ionic conductivity of the high-temperature hydrothermal crystals.

3.2. Defect and Damage Mechanisms. Applications of single-crystal KTP are limited by optical damage in the form of thin gray tracks produced by high-power, high-repetition-rate laser pulses.[101] The process of SHG

(98) Laudise, R. A. *Materials for Nonlinear Optics: Chemical Perspectives*; Marder, S. R., Sohn, J. E., Stucky, G. D., Eds.; ACS Symposium Series No. 445; American Chemical Society: Washington, DC, 1991; p 410.

(99) Morris, P. A.; Crawford, M. K.; Ferretti, A.; French, R. H.; Roelofs, M. G.; Bierlein, J. D.; Brown, J. B.; Loiacono, G. M.; Gashurov, G. *Mater. Res. Soc. Symp. Proc.* **1989**, *152*, 95.

(100) Morris, P. A.; Crawford, M. K.; Jones, B. *J. Appl. Phys.* **1992**, *72*, 5371.

(101) Scripsick, M. P.; Edwards, G. J.; Halliburton, L. E.; Belt, R. F.; Kappers, L. A. *SPIE Int. Soc. Opt. Eng.* **1991**, *1561*, 93.

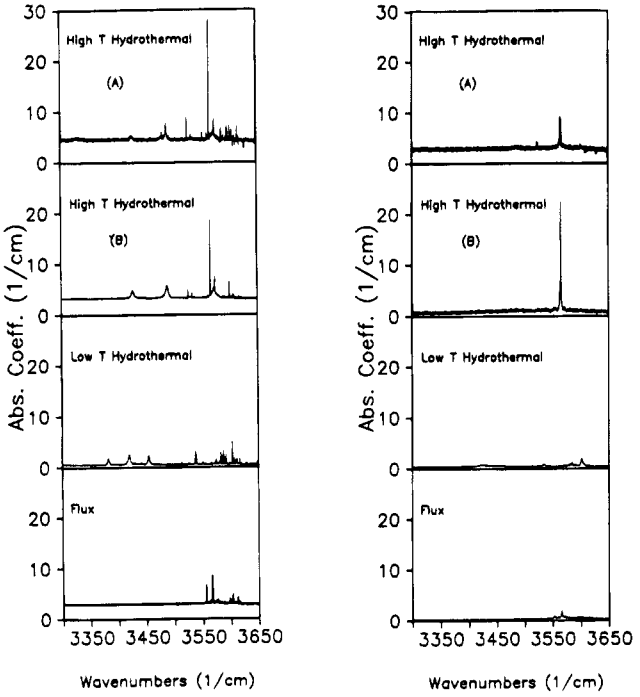

Figure 3.1. Infrared spectra of the high-temperature hydrothermal (HTA and HTB), low-temperature hydrothermal (LT), and flux (F1) KTP crystals at (a, left) 10 and (b, right) 300 K (incident radiation propagating along z; 0.1 cm^{-1} resolution). (Reprinted with permission from Morris et al.,[100] copyright 1992 American Institute of Physics.)

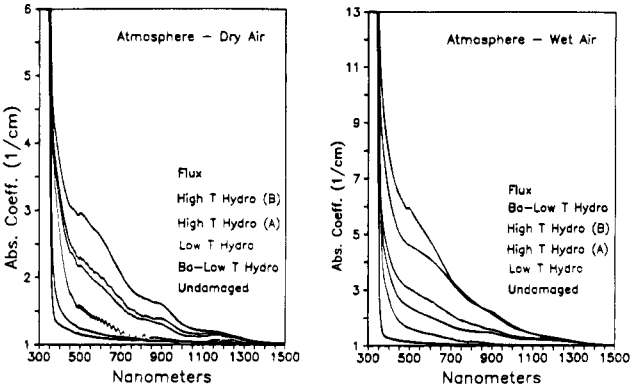

Figure 3.2. Optical absorption spectra of high-temperature hydrothermal and flux crystals which were electric-field damaged in dry and wet atmospheres. The absorption spectrum of an as-grown crystal is included for reference. (Reprinted with permission from Morris et al.,[87] copyright 1991 Int. Soc. Opt. Eng.)

in KTP crystals is accompanied by areas of high absorption of visible light leading to significant energy losses, decreased efficiency, and low damage threshold.[102] Color centers in KTP are a result of laser photoexcitation of the charge carriers with their subsequent capture at the impurity levels or at the defects of the crystalline lattice.[103] The identification of Ti^{3+} in KTP and its possible role in laser damage have been delineated by Roelofs.[104] Optical damage in KTP single crystals has been correlated to existing defect structures.[105] Two possible mechanisms for potassium vacancies in flux-grown KTP are interstitial potassium in a stoichiometric crystal or growth of a crystal deficient in K_2O leading to both potassium and oxide vacancies.[106] In either case, charge compensation for the Ti^{3+} centers, generated from the applied electric field, should be observed. Both scenarios are expected to be promoted by high-temperature growth.[104] A detailed study of the defect mechanisms of KTP along with effects of Ba doping on ionic conductivity has been completed.[87] Damage mechanisms depend on whether the crystals were electric-field damaged in dry or wet air atmospheres.[107] The results in wet air atmosphere are important for device application where ambient conditions are maintained. Optical absorption spectra of KTP crystals synthesized under various conditions and electric-field damaged in dry and wet environments are shown in Figure 3.2. The spectra indicate differences in relative damage susceptibilities. In wet atmospheres, the electric-field damage susceptibilites are correlated to ionic conductivity at room temperature. Also, large increases in OH^- defects occur in the more damaged materials. Therefore, it is believed that the primary damage mechanism under wet air conditions involves the introduction of protons into the crystals from the environment.

Morris and Crawford[107] have denoted the influence of water vapor on the susceptibility of KTP to electric-field damage. The susceptibilities of both hydrothermal and flux grown KTP crystals to electric-field-induced darkening increased with increasing water vapor in the atmosphere surrounding the crystals. Infrared spectroscopy indicated that Ti^{3+} defects generated by the applied electric field are charge compensated by hydrogen ions from the environment. The data presented strongly indicated that KTP-based photon electrooptical devices should be operated in a dry environment to reduce possible damage.

Point defects and their possible role in laser damage have also been examined by Scripsick et al.[101] Electron paramagnetic resonance studies identify platinum impurity centers, from the platinum crucibles used in the growth process, as possible contributors to gray tracking in KTP. The effect of temperature on SHG performance of KTP crystals has been studied.[108] Models of the photoexcitation process responsible for gray tracking are being explored. Cerium doping has been employed to reduce the optical absorption and creation of color centers in KTP.[109] Many of the observed defects in KTP crystals stem from the use of high processing temperatures. The effects of high-temperature processing of KTP are described in the following section.

3.3. High-Temperature Decomposition. The high-temperature decomposition and thermal instability of KTP below its melting point have been previously described.[21] $KTiOPO_4$ decomposes at an appreciable rate at elevated temperatures according to the net reaction

(102) Jacco, J. C.; Rockafellow, D. R.; Teppo, E. A. *Opt. Lett.* **1991**, *16*, 1307.
(103) Andreev, B. V.; Maslov, V. A.; Mikhailov, V. A.; Pak, S. K.; Shaunin, O. P.; Sherbakov, I. A. *SPIE Int. Soc. Opt. Eng.* **1991**, *1839*, 280.
(104) Roelofs, M. G. *J. Appl. Phys.* **1989**, *65*, 4976.
(105) Loiacono, G. M.; Stolzenberger, R. A. *Appl. Phys. Lett.* **1988**, *53*, 1498.
(106) Loiacono, G. M.; Loiacono, D. N.; McGee, T.; Babb, M. *J. Appl. Phys.* **1992**, *72*, 2705.
(107) Morris, P. A.; Crawford, M. K. *Appl. Phys. Lett.* **1993**, *62*, 799.
(108) Tyminski, J. *J. Appl. Phys.* **1991**, *70*, 5570.
(109) Blasse, G. *J. Alloys Compds.* **1993**, *194*, 139.

$$KTiOPO_4(s) \rightarrow (1 - \alpha)KTiOPO_4(s) + \alpha TiO_2(s) + \alpha/2(P_2O_5 + K_2O)(g)$$

where α represents the extent of decomposition. Powder X-ray diffraction (XRD) and scanning electron microscopy (SEM) coupled with energy-dispersive analysis by X-ray (EDAX) provided evidence for this description of the decomposition pathway (Figures 3.3 and 3.4, respectively). TiO_2 (rutile), the solid product of decomposition, was observed by both methods.

Microscopic investigation and kinetic analysis revealed that the decomposition developed on the surface of KTP microcrystals. The high-temperature behavior of KTP can be used to explain the need to renew the surface of a seed crystal before initiation of crystal growth[20] and should be taken into account for any KTP ceramic technology or method of KTP thin-film deposition. It has been shown that if crystalline films of KTP are desired, any procedure involving heat treatment to improve thin-film crystallinity must not require high temperatures. A high-temperature anneal would ultimately lead to the destruction of the film or the generation of microcrystallites that would act as light scatterers and reduce the film's transparency.

A practical understanding of the structure and processing–defect–property relationships in KTP has proven crucial in the fabrication of KTP waveguides. Section 4 focuses on the development of waveguides based on KTP single crystals.

4. KTP Waveguides

An optical waveguide is a light conduit consisting of a strip, slab, or cylinder of dielectric material surrounded by another dielectric material of lower refractive index (Figure 4.1).[110] The light is confined and transported through the inner medium without radiating into the surrounding medium. The concept of optical confinement is relatively simple. A medium of one refractive index embedded in a medium of a slightly lower refractive index acts as a light trap within which optical waves are confined through multiple internal reflections at the waveguide boundaries. The angle of the incident light coupled with the difference in refractive indexes controls the total internal reflection condition. Consequently, the geometry of the waveguide strongly influences light interactions and device design. The principal advantage of optical waveguides lies in their confinement of light. The confinement of light in a micrometer-sized waveguide and its propagation without appreciable diffraction greatly increases the optical fields and the efficiencies of NLO processes.[111]

One type of waveguide consists of a nonlinear optical crystal onto whose surface a dopant has been applied forming a channel or planar region with a higher refractive index.[2] Light which enters this channel is totally internally reflected as a result of the refractive index difference between the inside and outside of the channel. Useful geometries for channel waveguides are shown in Figure 4.2.[110] Waveguides may be fabricated in different configurations, as illustrated in Figure 4.3 for the embedded-strip geometry. S bends are used to offset the propagation axis while the Y branch plays a crucial role as a beamsplitter or combiner. Two Y branches may be utilized to form a Mach-Zehnder interferometer, and two waveguides in close proximity (or intersecting) can exchange power and be used as directional couplers.[110] Light can also be manipulated by changes in refractive index induced by an applied electric field. Electrooptic modulation is inherently nonlinear and is the foundation of many dynamic guided wave optical devices (Mach-Zehnder interferometers, channel switches, and directional couplers) essential for fiber optic communications. In waveguide devices, light can be more efficiently and effectively controlled compared to bulk-optic devices because the interaction between light and an externally applied signal is restricted to the region surrounding the waveguide. Devices made from optical waveguides have enhanced design flexibility.[112]

KTP channel waveguides have superior qualities such as sharp depth profiles and minimal lateral diffusion that make them ideal for various NLO device applications.[113] KTP has a waveguide figure-of-merit (FOM) that is nearly double that of any other inorganic material.[5] Table 4.1 compares various materials used as waveguide electrooptical modulators.[85] KTP has an extremely high potential for integrated optic applications provided that low-loss optical waveguides can be easily fabricated.[5]

4.1. Fabrication and Design. Waveguide structures for effective second harmonic conversion and other NLO applications have been successfully fabricated using standard ion exchange of KTP single crystals.[114] KTP waveguides are currently fabricated by sputtering a thin film of Al, Au, or Ti onto the (001) surface of a cut and polished KTP single crystal, removing a narrow strip of this film, and exposing the surface to molten nitrate salts of various metals (Rb^+, Cs^+, Tl^+) between 350 and 450 °C.[2] Typical exposure time ranges from 3 to 4 h. The ion-exchanged waveguides are stable at room temperature and in accelerated aging tests.[114] Provided that the diffusion processing temperature remains below 450 °C, the exchange process does not introduce detectable surface defects.

A fundamental understanding of the ion-exchange process has been provided by Roelofs and co-workers.[115] The introduction of divalent cations increased the low-frequency dielectric constants and loss in KTP by several orders of magnitude. These results further substantiate a potassium vacancy mechanism for ionic conductivity. In the case of univalent exchange, careful control of the metal ratio in the melt can be utilized to obtain various mixed-metal waveguides whose index can be smoothly adjusted between the extremes of the pure crystals. Table 4.2 provides typical waveguide characteristics.[114] The maximum increase in refractive index was observed for Tl^+. Note also that ionic diffusion was more favorable along the *c* axis again revealing the

(110) Saleh, B. E. A.; Teich, M. C. *Fundamentals of Photonics*; Wiley and Sons, Inc.: New York, 1991.
(111) Roelofs, M. G.; Ferretti, A.; Bierlein, J. D. *J. Appl. Phys.* **1993**, *73*, 3608.
(112) Waynant, R. W., Ediger, M. N., Eds. *Electro-Optics Handbook*; McGraw-Hill, Inc.: New York, 1994.
(113) Bierlein, J. D.; Laubecher, D. B.; Brown, J. B.; van der Poel, C. J. *Appl. Phys. Lett.* **1990**, *56*, 1725.
(114) Bierlein, J. D.; Ferretti, A.; Brixner, L. H.; Hsu, W. Y. *Appl. Phys. Lett.* **1987**, *50*, 1216.
(115) Roelofs, M. G.; Morris, P. A.; Bierlein, J. D. *J. Appl. Phys.* **1991**, *70*, 720.

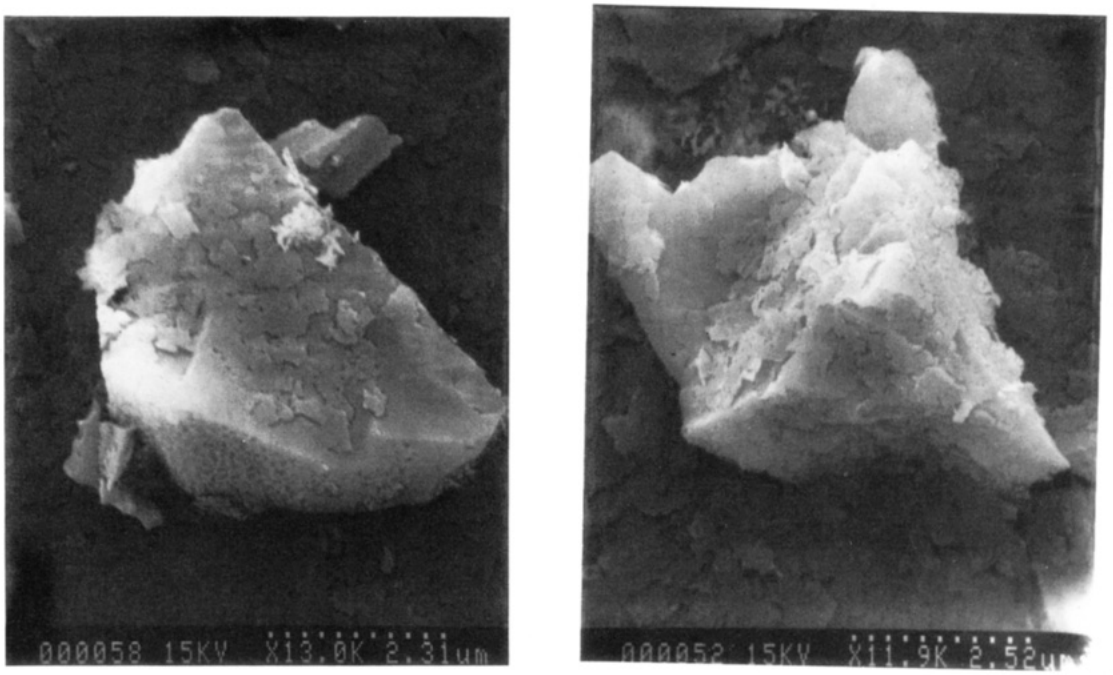

Figure 3.3. SEM micrographs of KTP microcrystals at early and late stages of decomposition. (Reprinted with permission from Hagerman et al.,[21] copyright 1993 American Chemical Society.)

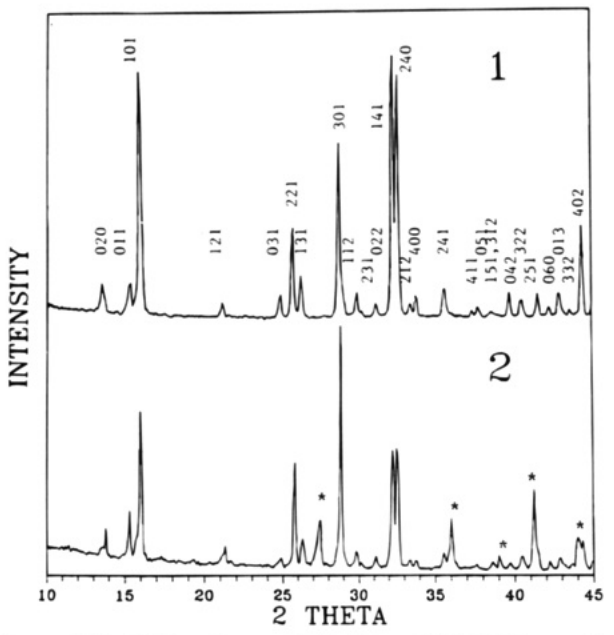

Figure 3.4. XRD patterns of 91) sintered $KTiOPO_4$ powder; (2) KTP powder after heat treatment at 1050 °C in a nitrogen atmosphere. Asterisks mark peaks belonging to TiO_2 (rutile). (Reprinted with permission from Hagerman et al.,[21] copyright 1993 American Chemical Society.)

anisotropy of ionic conductivity. The channel guides formed by this process are characterized by very sharp boundaries at the edge of the guide and high uniformity across the guide.[6] Figure 4.4 shows an SEM micrograph of a KTP segmented waveguide.[113] The sharp edges of the waveguide shown clearly in this figure provide further evidence of the highly anistropic ion exchange process in KTP. This anisotropy is essential for minimizing lateral diffusion and is a direct consequence of the KTP structure.[116]

Anisotropic diffusion has significant advantages for NLO device fabrication: realization of high-index guide arrays and modulated index guides, optimization of

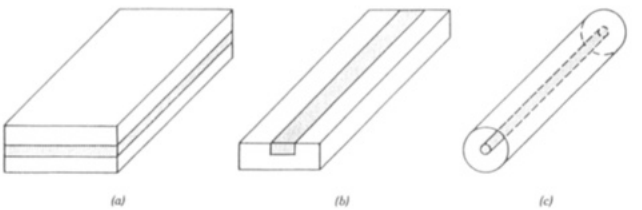

Figure 4.1. Optical waveguides: (a) slab; (b) strip; 9c) fiber. (Reprinted with permission from Saleh et al.,[110] copyright 1991 Wiley and Sons, Inc.)

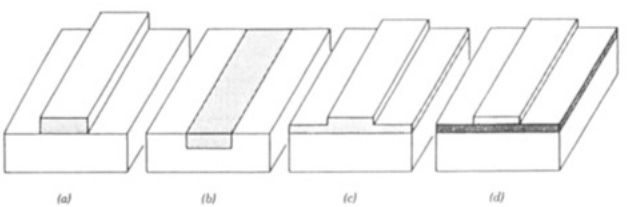

Figure 4.2. Various types of waveguide geometries: (a) strip; (b) embedded strip; (c) rib or ridge; (d) strip loaded. The darker the shading, the higher the refractive index. (Reprinted with permission from Saleh et al.,[110] copyright 1991 Wiley and Sons, Inc.)

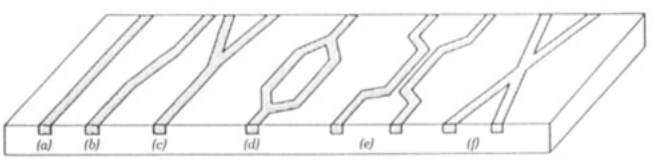

Figure 4.3. Different configurations for waveguides: (a) straight; (b) S bend; (c) Y branch; (d) Mach–Zehnder; (e) directional coupler; (f) intersection. (Reprinted with permission from Saleh et al.,[110] copyright 1991 Wiley and Sons, Inc.)

electric-field overlap for switches and modulators, and optimization of optical-field overlap for integrated optical applications.[85] Figure 4.5 shows a Tl-exchanged optical waveguide in KTP.[116] Figure 4.6 provides an end

(116) Bierlein, J. D.; Ferretti, A.; Roelofs, M. G. *SPIE Int. Soc. Opt. Eng.* **1988**, *994*, 160.

Table 4.1. Electrooptical Waveguide (FOM) for Inorganic Materials (After Bierlein et al.[85])

	r (pm/V)	n	ϵ_{eff}	n^3r/ϵ_{eff} (pm/V)
KTP, r_{33}	35	1.86	13	17.3
$KNbO_3$, r_{33}	27	2.17	30	9.2
$LiNbO_3$, r_{33}	29	2.20	37	8.3
$Ba_2NaNb_5O_{15}$	56	2.22	86	7.1
KTP, r_{23}	14	1.76	13	5.9
SBN(25–75)	56–1340	2.22	119–3400	5.1–0.14
GaAs	1.2	3.6	14	4.0
$LiNbO_3$, r_{13}	10	2.29	37	3.2
$BaTiO_3$	28	2.36	373	1.0

Table 4.2. Waveguide Characteristics of $KTiOPO_4$ (After Bierlein et al.[116])

ion	surface type	temp (°C)	time (h)	no. of modes	mode type	d (μm)	Δn
Rb	X	450	3.3	0	TE		
				1	TM	1.3	0.02
Rb	Z(+)	350	4	3	TE	4.0	0.019
				3	TM	4.0	0.018
Rb	Z(−)	350	4	3	TE	6.5	0.008
				2	TM	6.5	0.008
Cs	Z	450	4	11	TE	13	0.028
				8	TM	13	0.019
Tl	Z	335	4	4	TE	1.6	0.23
				4	TM	1.6	0.18

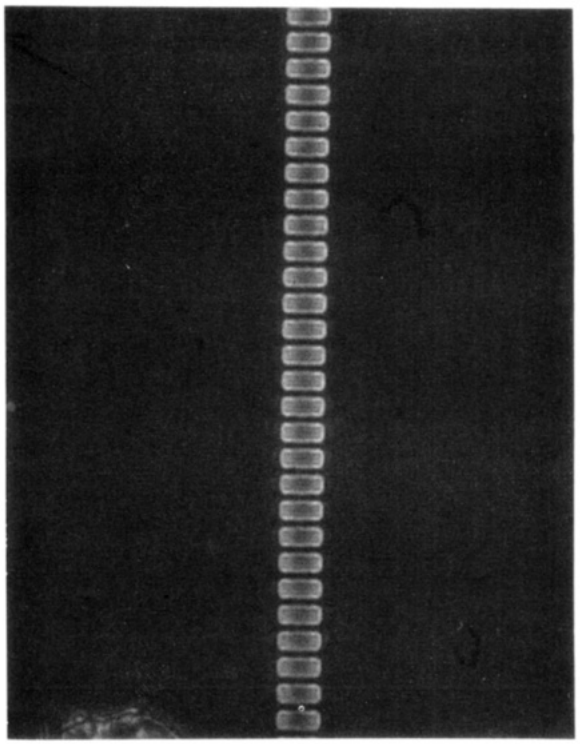

Figure 4.4. Top view of a 4 μm period Rb-exchanged KTP segmented waveguide. (Reprinted with permission from Bierlein et al.,[113] copyright 1990 American Institute of Physics.)

view of Rb–Ba channel waveguide in KTP.[116] The ion diffusion is confined within discrete channels, and essentially no lateral diffusion is observed for the 6 μm guide with a depth near 100 μm. This confinement is in direct contrast with Ti:$LiNbO_3$ waveguides in which regions of Ti doping tend to stray outside of the intended waveguide boundary.[2] Optical waveguides in KTP can also be fabricated by proton or ammonium exchange.[111] The index profiles of proton exchanged guides are more steplike than Rb-exchanged guides, suggesting the formation of proton-enriched phases also present in lithium niobate guides.

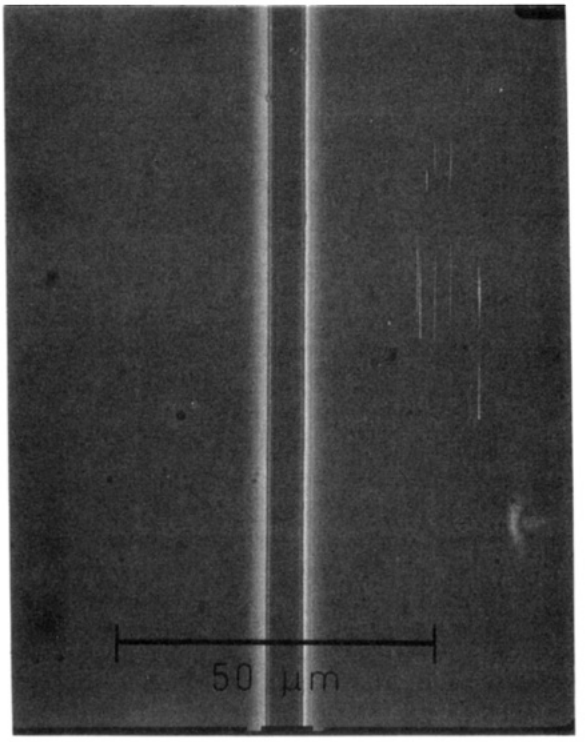

Figure 4.5. Tl-exchanged KTP waveguide. (Reprinted with permission from Bierlein et al.,[116] copyright 1988 Int. Soc. Opt. Eng.)

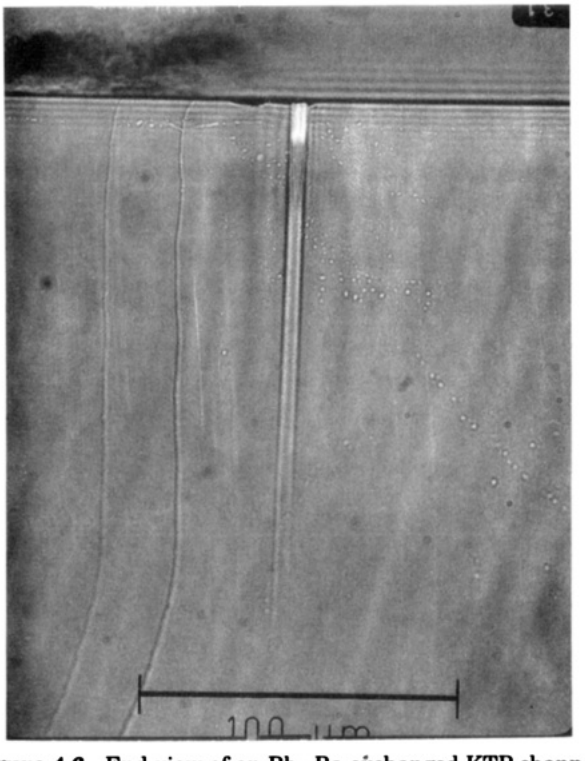

Figure 4.6. End view of an Rb–Ba exchanged KTP channel waveguide. (Reprinted with permission from Bierlein et al.,[116] copyright 1988 Int. Soc. Opt. Eng.)

4.2. Device Applications. KTP has been recognized as a superior material for guided wave optics.[113] Current devices made from KTP waveguides have included a single-channel phase modulator[85] and a Mach–Zehnder interferometer.[117] Balanced phase matching (BPM) in segmented KTP waveguides has been reported by Bierlein et al.[113] This new phase-

matching technique has proven effective in mixed bulk waveguide systems using KTP with a SHG conversion efficiency of 15%/W/cm^2 at 1.064 μm. Strategies to increase waveguide refractive index by tightening mode confinement and increasing conversion efficiency were employed. The BPM technique can significantly improve the processing latitude of practical NLO devices based on KTP guides.[113] van der Poel et al.[118] have reported type I phase-matched blue SHG from periodically segmented channel ion-exchanged KTP waveguides. (For a detailed description of the optical physics of KTP including type I and type II phase matching, consult Stucky et al.[2]) These guides yielded output wavelengths ranging from 0.38−0.48 μm and efficiencies exceeding 50%/W/cm^2. Experiments involving surface SHG, electrostatic tuning, selective etching, and piezoelectric measurements have indicated that the origin of the large type I conversion efficiencies was ferroelectric domain reversal induced by the waveguide processing conditions.[119] Specifically, ferroelectric domain reversal has been observed in waveguides fabricated through ion exchange with Ba. Ion-exchange experiments with different substrate materials and surface polarities, and a variety of molten salt compositions are under investigation to optimize conversion efficiency and to clarify the mechanism of domain reversal in these materials.[118] Domain reversal techniques have also been employed in the fabrication of $LiNbO_3$ and $LiTaO_3$ channel waveguides.[120]

Compact sources of blue-green light are of interest for a variety of applications. Guided wave frequency up-converters have the potential for higher efficiency compared to bulk devices because the interacting waves can be confined to a small area over a longer length than in bulk devices where confinement is limited by diffraction. Two infrared input frequencies and combinations of SFG and SHG of segmented optical waveguides fabricated through standard ion-exchange techniques have been used for the simultaneous generation of ultraviolet, blue and green light.[121−125] Through further optimization of this technique, it appears possible to generate milliwatts of power at several wavelengths, simultaneously. KTP waveguides are also being investigated for frequency up-conversion of strained-layer InGaAs lasers in the 0.9−1.0 μm range.[126] To solve phase-matching problems for the generation of compact blue light laser source, grating structures involving periodic reversal of the phase of the nonlinear generated wave are employed (quasi-phase-matching, QPM).[119] Segmented KTP waveguides designed for QPM frequency doubling have a periodic variation in refractive index that acts as a distributed Bragg reflector (DBR).[127] Practical blue light laser sources require techniques such as QPM and DBR to provide stabilization of the infrared laser beam and to optimize output efficiencies.[128,129]

To create ultrahigh-speed long-distance optical fiber communications systems and implement optical information processing systems, various devices having less than 10 ps high-speed characteristics are required.[130] Buritskii and co-workers have proposed the use of KTP based waveguides for all-optical switching. The passing of subnanosecond light pulses through Rb−KTP nonlinear directional coupler has been achieved with nonlinear switching of 40% of the input light power (5 kW). Chu and co-workers have reported that Tl-exchanged KTP possesses both acoustic and optical waveguiding properties.[131] The photorefractive effect, important for optical switching devices, has been examined for Rb ion-exchanged KTP waveguides.[132] KTP shows a very high potential for optically driven integrated devices and may become the material of choice for high-speed information processing.

Because of enhanced design flexibility and capability, as well as lower cost, KTP waveguides based on thin-film fabrication may offer an attractive alternative compared to existing waveguides based on single-crystal ion-exchange methods. To date, however, work on the fabrication of KTP thin films and the subsequent development of NLO devices based on these thin films are relatively unexplored; see section 5.

5. KTP Thin Films

As discussed in section 4, waveguide structures for effective second harmonic conversion and other photonic applications have been successfully fabricated using standard ion-exchange of $KTiOPO_4$ single crystals. However, the development of waveguide devices based on potassium titanyl phosphate thin films may offer a more easily implementable strategy for existing device structures. Wu states:[133] "Thin films are important for realizing integrated optical devices (such as spatial light modulator, directional coupler, and total internal reflection waveguide switch) for applications in optical computing, signal processing, wave mixing, and beam steering. In an integrated device, the semiconducting light source, electrooptical thin-film waveguide, and semiconducting light detector can all be fabricated and built on the same substrate provided that the thin-film deposition and fabrication process are compatible with that of the semiconducting materials." Moreover, KTP films fabricated on non-KTP substrates could provide a low-cost route to novel photonic applications not yet considered because of the problems and restraints incurred with existing single-crystal technologies (bulk damage effects, size and geometry constraints).

(117) Laubacher, D. B.; Guerra, V.; Chouinard, M. P.; Liou, J.; Wyant, P. *SPIE Int. Soc. Opt. Eng.* **1988**, *993*, 80.
(118) van der Poel, C. J.; Bierlein, J. D.; Brown, J. B.; Colak, S. *Appl. Phys. Lett.* **1990**, *57*, 2074.
(119) Laurell, F.; Roelofs, M. G.; Bindloss, W.; Hsiung, H.; Suna, A.; Bierlein, J. D. *J. Appl. Phys.* **1992**, *71*, 4664.
(120) Makio, S.; Nitanda, F.; Kohei, I.; Sato, M. *Appl. Phys. Lett.* **1992**, *61*, 3077.
(121) Jongerius, M. J.; Bolt, R. J.; Sweep, N. A. *J. Appl. Phys.* **1994**, *75*, 3316.
(122) Laurell, F.; Brown, J. B.; Bierlein, J. D. *Appl. Phys. Lett.* **1993**, *62*, 1872.
(123) Laurell, F. *Electron. Lett.* **1993**, *29*, 1629.
(124) Laurell, F.; Brown, J. B.; Bierlein, J. D. *Appl. Phys. Lett.* **1992**, *60*, 1064.
(125) Zhang, L.; Chandler, P. J.; Townsend, P. D.; Alwahabi, Z. T.; Pityana, S. L.; McCaffery, A. J. *J. Appl. Phys.* **1993**, *73*, 2695.
(126) Risk, W. P.; Nadler, Ch. K. *SPIE Int. Soc. Opt. Eng.* **1991**, *1561*, 130.
(127) Risk, W. P.; Lau, S. D. *Opt. Lett.* **1993**, *16*, 272.
(128) Hagan, D. J.; Wang, Z.; Stegeman, G.; Van Stryland, E. W.; Sheik-Bahae, M.; Assanto, G. *Opt. Lett.* **1994**, *19*, 1305.
(129) Sundheimer, M. L.; Villeneuve, A.; Stegeman, G. I.; Bierlein, J. D. *Electron. Lett.* **1994**, *30*, 1400.
(130) Buritskii, K. S.; Dianov, E. M.; Maslov, V. A.; Chernykh, V. A.; Scherbakov, E. A. *Appl. Phys. B.* **1992**, *54*, 167.
(131) Chu, D. K. T. *Appl. Phys. Lett.* **1994**, *65*, 1989.
(132) Shi, L. P.; Karthe, W.; Rasche, A. *Appl. Phys. Lett.* **1994**, *65*, 2539.
(133) Wu, A. Y. *4th Int. SAMPE Elect. Conf. Proc.* **1990**, 722.

5.1. Magnetron Sputtering. Work by Wu[133] using radio-frequency magnetron sputtering (RFMS) to deposit KTP thin films on fused silica resulted in predominately amorphous films even at substrate temperatures as high as 650 °C. While RFMS is a remarkably successful physical vapor deposition technique which has been shown to be effective in the deposition of thin films of a variety of electrooptical and nonlinear optical thin films (including PLZT, $BaTiO_3$, and β-BaB_2O_4), it is possible that sputtering may not be the optimum technique for the deposition of KTP thin films. Some methods of film deposition, such as magnetron sputtering, inevitably require elevated temperatures near the target. Owing to the nature of the defect chemistry and high-temperature decomposition discussed previously in section 3, it is important to understand the requirement that the thin films be fabricated at temperatures below 900 °C. Recent successes in KTP thin film fabrication have involved existing single-crystal synthesis technology (liquid phase epitaxy) or procedures which do not rely on extremely high processing temperatures (sol–gel and pulsed excimer laser ablation).

5.2. Liquid-Phase Epitaxy. Thin films of $KTiOP_xAs_{1-x}O_4$ were grown by Cheng et al. on KTP substrates by liquid-phase epitaxy using a tungstate flux.[63] Optical waveguiding at 0.633 μm was demonstrated in a 20 μm thick $KTiOP_{0.76}As_{0.24}O_4$ film fabricated on a [011] KTP substrate. The refractive index difference in the film relative to the KTP substrate, Δn, was calculated to be approximately 0.012. Cheng and co-workers[134] have noted that other substrate materials with more favorable properties could be utilized. In principle, any crystal which has the appropriate lattice match and is chemically stable under the reaction conditions could be used. Optimally, one should look for a crystal with the following properties: congruent melting, low dielectric constant and refractive index, and negligible ionic conductivity. $K(Mg_{0.33}Nb_{0.67})OPO_4$ (KMNP) has been examined as a possible substrate for KTP and KTA.[135]

Energy-dispersive X-ray spectrometry (EDS) was performed to confirm that there was no in-diffusion of arsenic into the substrate. A typical EDS scan showing the atomic profiles is given in Figure 5.1. The EDS spectra revealed an abrupt increase in the arsenic concentration at the film–substrate interface and thus suggested an abrupt, steplike refractive index profile. Importantly, the steplike refractive index profile exhibited in these epitaxially grown waveguides is not limited to the anionic phosphate–arsenate solid solution. Appropriate replacement of the titanyl group via solid solution formation (e.g., Sn) or impurity doping (e.g., Cr) could generate epitaxial films with well-defined refractive index boundaries.

The potential uses of the planar $KTiOP_xAs_{1-x}O_4$ waveguides are discussed by Cheng et al.[63] along with possible device structures based on these films. More specifically, these films offer advantages in device fabrication and applications when compared to RTP channel waveguides discussed in section 4. A substantial problem with the fabrication of RTP channel

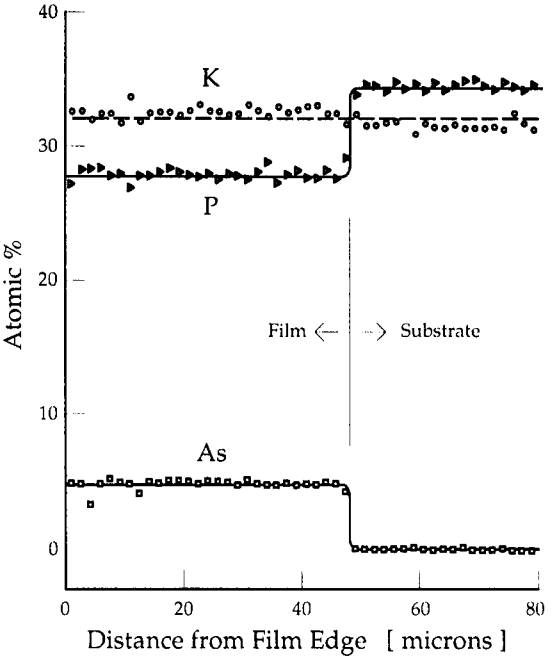

Figure 5.1. EDS data for 50 μm $KTiOP_xAs_{1-x}O_4$ waveguide. Titanium content is not shown for clarity. Spatial resolution of EDS is approximately 0.5 μm. (Reprinted with permission from Cheng et al.,[63] copyright 1991 American Institute of Physics.)

waveguides is the difficulty in controlling the waveguide depth and corresponding dispersion. The authors offer a solution to this problem by proposing the deep Rb ion exchange of these epitaxial films. Current results indicate that the step-index profile of the film promotes effective confinement of light within the epitaxial layer. This type of confinement will make the device insensitive to the refractive index fluctuation caused by the ion-exchange process. Future work on the development of similar waveguide structures with a sigmoidal refractive index profile is under investigation to enhance design flexibility and optimize device performance.[63]

5.3. Sol–Gel. A new route to forming thin films of KTP using sol–gel chemistry is described by Harmer and Roelofs.[136] The authors describe the relevant precursor chemistry, film formation, microstructural characterization, and waveguiding properties. The potential advantages of utilizing the sol–gel technique in thin film fabrication include: (i) good compositional control; (ii) homogeneity resulting from an intimate mixing of all precursors; (iii) low processing temperatures; (iv) easier fabrication of large-area thin films; (v) low cost.

Precursor solutions were prepared by Harmer et al. using the aqueous hydrolysis condensation reaction of the corresponding alkoxides. Bulk samples of KTP were prepared by evaporation of the solvent from the precursor solution and subsequent calcination of the solid produced. A spin-coating technique was employed to fabricate thin films of potassium titanyl phosphate on quartz, silicon, and lanthanum aluminate substrates. X-ray diffraction studies revealed that crystallization occurred at temperatures greater than 500 °C (see Figure 5.2). Below this temperature, KTP films prepared by the sol–gel technique showed poor crystallity.

(134) Cheng, L. K.; Bierlein, J. D.; Foris, C. M.; Ballman, A. A. *J. Cryst. Growth* **1991**, *112*, 309.
(135) McCarron, E. M., III.; Calabrese, J. C.; Gier, T. E.; Cheng, L. K.; Foris, C. M.; Bierlein, J. D. *J. Solid State Chem.* **1993**, *102*, 354.
(136) Harmer, M. A.; Roelofs, M. G. *J. Mater. Sci. Lett.* **1993**, *12*, 489.

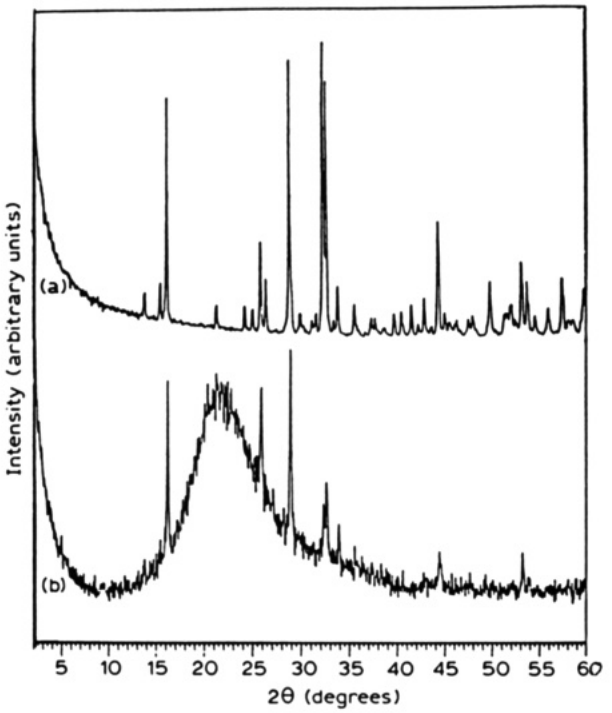

Figure 5.2. X-ray diffraction patterns of calcined KTP precursor for: (a) a bulk sample; (b) a thin-film grown on polycrystalline quartz and calcined at 750 °C in air for 10 h. (Reprinted with permission from Harmer et al.,[136] copyright 1993 Chapman and Hall.)

Scanning electron microscopy (SEM) was utilized to examine film microstructure and thickness. The KTP films were continuous and crack-free with a thickness of about 0.1 μm. Figure 5.3 shows a typical SEM micrograph of a thin film grown on polycrystalline quartz and calcined at 750 °C. The apparent density was greater than 90% with a grain size in the region of 0.3 μm. The processing conditions (heating rate, temperature, and annealing time) influenced the observed microstructure. Waveguiding was observed using a prism coupling method.[136] One film supported two optical modes for both TE and TM polarizations, with effective indexes increased over those of silica (n = 1.459) by $\Delta n_{TE_0} = 0.250(3)$, $\Delta n_{TM_0} = 0.268(3)$, $\Delta n_{TE_1} = 0.132(3)$, and $\Delta n_{TM_1} = 0.138(3)$. The average refractive index of the film was $n = 1.75$. The optical studies support a slight c-axis alignment of the crystallites. A more detailed study of the influence of processing conditions on film microstructure and waveguiding is currently in progress.[136]

5.4. Pulsed Excimer Laser Ablation. An outstanding review of pulsed laser deposition (PLD) has been provided by Saenger.[137] PLD has been widely used for the deposition of high-quality thin films of a variety of materials including high-T_c superconducting metal oxides, diamond-like carbon, superlattice structures, and, more recently, nonlinear optical mixed-metal oxides. The reviewer supplied a comprehensive list of materials deposited by PLD and discussed the differences between various PLD techniques including pulsed excimer laser ablation (PELA). Specifically, the success of the PELA technique is based on the following unique features: (i) replication of complex target stoichiometry;

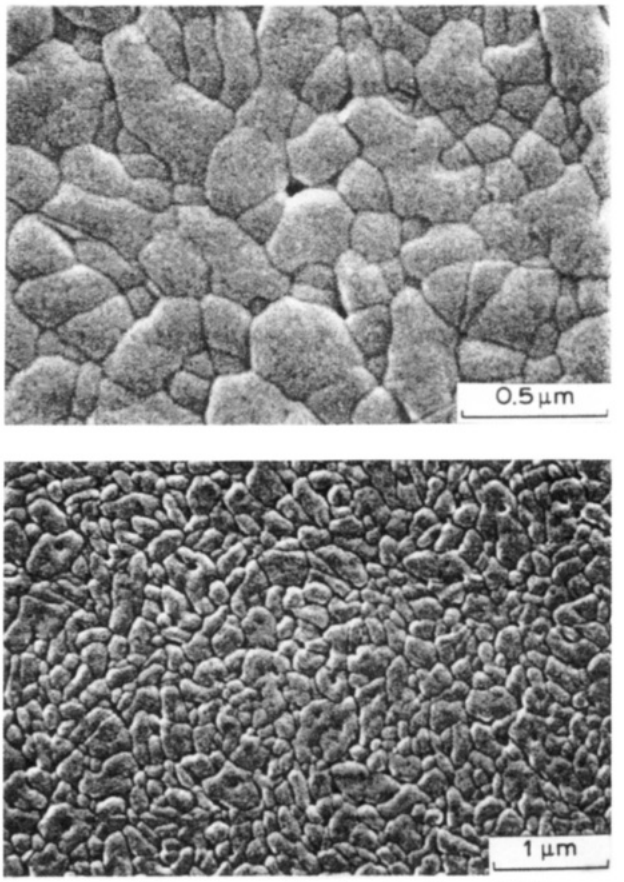

Figure 5.3. SEM micrographs of a thin film of KTP grown on polycrystalline quartz nd calcined at 750 °C, with a film thickness of about 0.6 μm, at different magnifications. (Reprinted with permission from Harmer et al.,[136] copyright 1993 Chapman and Hall.)

(ii) nonselective evaporation; (iii) high photon-enhanced ionization. Saenger concludes that further advancement in the understanding of the interrelationships between process characteristics and thin-film properties is of primary concern. Moreover, the phenomenology and mechanisms of PLD were described in a second review.[138] Discussions of target morphology, plume diagnostics, laser-plume interactions, and composition uniformity provided delineation of process mechanisms. An insightful diagram of the mechanisms of particulate production was given by Saenger (Figure 5.4). Schemes of particulate reduction were also provided by Saenger[137] and summarized in Figure 5.5.

Nonlinear optical thin films of potassium titanyl phosphate have been successfully fabricated by pulsed excimer laser ablation on substrates of sapphire, silicon, and fused quartz.[139] The films deposited on sapphire substrates in the temperature range 450–550 °C showed high crystallinity with preferential orientations, (100) and (011) (Figure 5.6). The substrate temperature and the oxygen partial pressure strongly influenced the observed crystallinity and transparency. Growth on silicon and quartz substrates was polycrystalline. The stoichiometry of the films was found to be titanium rich by Rutherford backscattering spectroscopy (RBS). Confirmation of titanium-rich films was provided by energy-

(137) Saenger, K. L. *Proc. Adv. Mater.* **1993**, *2*, 1.

(138) Saenger, K. L. *Proc. Adv. Mater.* **1993**, *3*, 63.

(139) Xiong, F.; Chang, R. P. H.; Hagerman, M. E.; Kozhevnikov, V. L.; Poeppelmeier, K. R.; Zhou, H.; Wong, G. K.; Ketterson, J. B.; White, C. W. *Appl. Phys. Lett.* **1994**, *64*, 161.

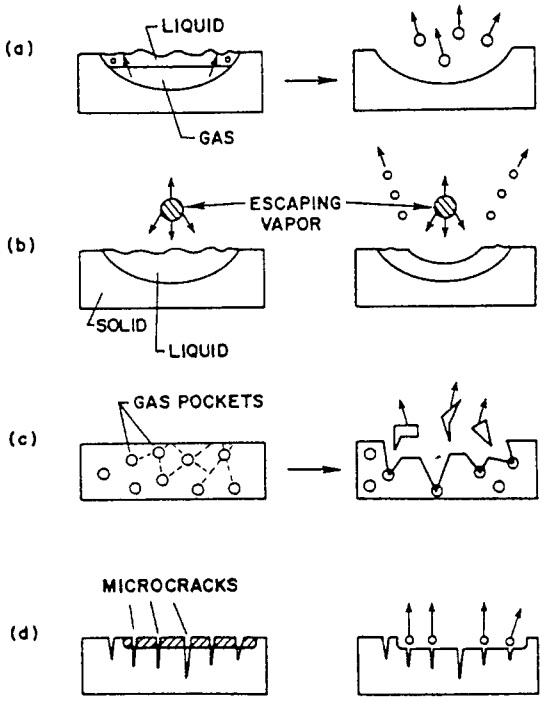

Figure 5.4. Mechanisms of particulate production: (a) splashing; (b) recoil pressure; (c) target outgassing; (d) fracto emission. (Reprinted with permission from Saenger,[138] copyright 1993 Chapman and Hall.)

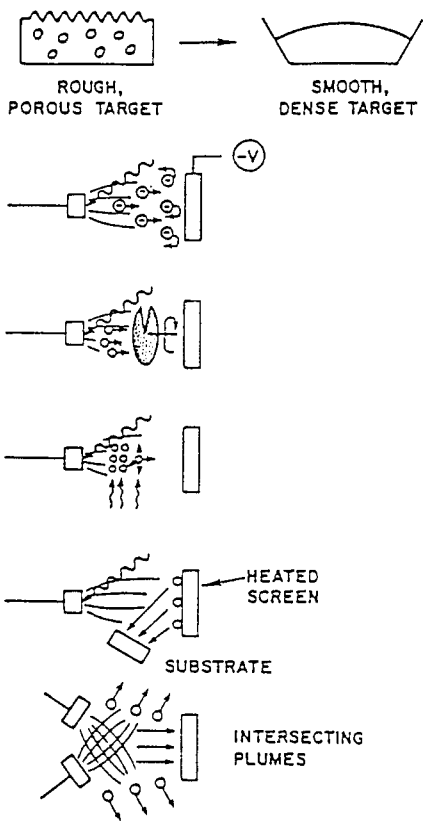

Figure 5.5. Schemes of particulate reduction: (a) high-density or liquid target; (b) electrostatic deflections; (c) mechanical chopping; (d) in-flight vaporization by a secondary laser pulse; (e) heated screen; (f) intersecting plumes. (Reprinted with permission from Saenger,[137] copyright 1993 Chapman and Hall.)

dispersive analysis by X-rays (EDAX). The average refractive indexes of the films evaluated by spectroscopic ellipsometry (SE) in the spectral region 0.3–0.9 μm

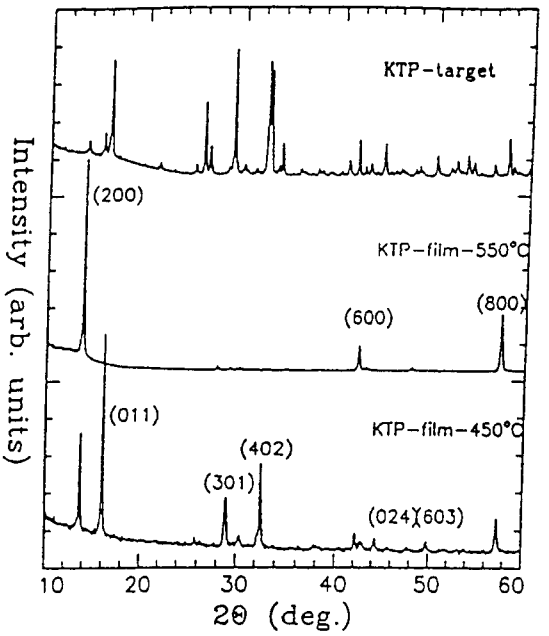

Figure 5.6. X-ray diffraction patterns of (a) KTP target; (b) KTP film grown on sapphire and deposited at 550 °C; 9c) KTP film grown on sapphire and deposited at 450 °C. (Reprinted with permission from Xiong et al.,[139] copyright 1994 American Institute of Physics.)

ranged from 1.75 to 2.00 and were consistent with the known bulk values. The sapphire deposited film exhibited a high nonlinear optical response with a calculated d_{eff} approximately 10% of the bulk value of single-crystal KTP.

X-ray diffraction studies coupled with optical analysis support a slight a-axis alignment of the KTP crystallites. Xiong et al. concluded that the congruent evaporation and high kinetic energy of the ablated species associated with the PELA process minimize the probability of decomposition and thus enhance stoichiometric conversion and promote the successful deposition of crystalline KTP films. Research continues on the development of KTP waveguides based on PELA films.[140] Strategies for the development of highly crystalline KTP films on amorphous substrates of low refractive index are being employed along with the use of high-density KTP ceramic to enhance film morphology and crystallinity. Highly textured KTP thin films on fused quartz substrates with optical nonlinearities approximately one-third the value of the largest component in single-crystal KTP have recently been reported by Lundquist et al.[141] The SHG frequency dispersion of KTP thin films on fused quartz was determined and found to be uniform for visible second harmonic wavelengths. Lundquist and co-workers observed endfire coupling in planar KTP guides with propagation losses of less than 1 dB/cm. Novel photonic devices based on KTP thin-film optical waveguides are discussed in section 6.

6. NLO Devices Based on KTP Thin Films: A New Strategy

Integrated optics is the technology of integrating various optical devices and components for the genera-

(140) Xiong, F.; Hagerman, M.; Zhou, H.; Kozhevnikov, V.; Poeppelmeier, K. R.; Ketterson, J. B.; Chang, R. P. H.; White, C. W. *J. Vac. Sci. Technol. A* **1994**, *12*, 1446.

(141) Lundquist, P. M.; Zhou, H.; Hahn, D. N.; Ketterson, J. B.; Wong, G. K.; Hagerman, M. E.; Poeppelmeier, K. R.; Ong, H. C.; Xiong, F.; Chang, R. P. H. *Appl. Phys. Lett.*, in press.

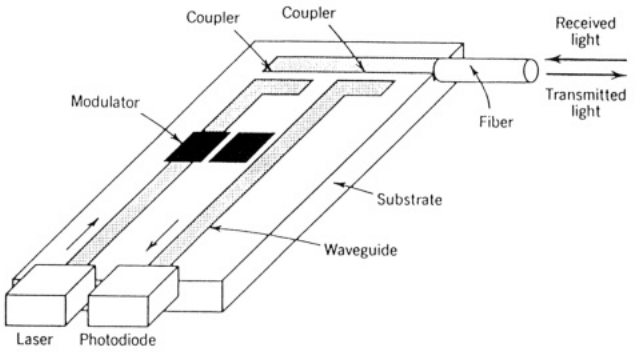

Figure 6.1. Example of an integrated optic device used as an optical receiver/transmitter. (Reprinted with permission from Saleh et al.,[110] copyright 1991 Wiley and Sons, Inc.)

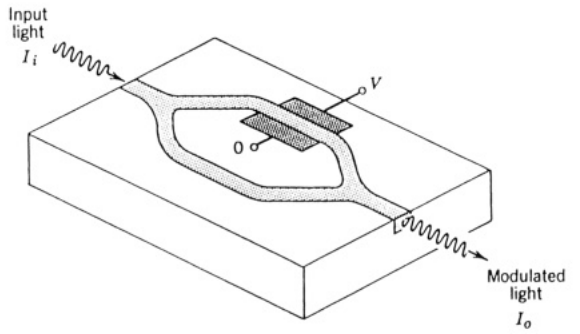

Figure 6.2. Integrated optical intensity modulator (or optical switch). (Reprinted with permission from Saleh et al.,[110] copyright 1991 Wiley and Sons, Inc.)

tion, focusing, splitting, combination, isolation, polarization, coupling, switching, modulation, and detection of light, all on a single substrate.[110] Optical waveguides serve as the essential connections between these components. An optical integrated circuit (OIC) is a thin-film type optical circuit designed to perform a function by integrating a laser diode light source, functional components such as switches/modulators, interconnecting waveguides, and photodiode detectors, all on a single substrate.[112] Through hybrid integration, a more compact, stable, and functional optical system can be produced. The key components are slab and channel waveguides. Therefore, the crucial point in the development of an OIC is the design and fabrication of high-quality waveguides using optimal materials and processes. The important features of OIC's include:[112] (i) single-mode structure with waveguide widths on the order of micrometers; (ii) stable alignment by integration leading to enhanced vibration and temperature tolerances; (iii) easy control of the guided wave; (iv) low operating voltage and short interaction length; (v) faster operation owing to shorter electrodes and less capacitance; (v) larger optical power density; (vi) compactness and light weight.

An example of an integrated optic device used as an optical receiver/transmitter[110] is shown in Figure 6.1. Received light is coupled into a waveguide and directed to a photodiode where it is detected. The laser light is then guided, modulated, and coupled into an optical fiber. Another important integrated optic device is the intensity modulator or optical switch (see Figure 6.2). A Mach–Zehnder interferometer and an elecrooptic phase modulator are coupled using optical waveguides.

6.1. Development and Implementation. The development and implementation of nonlinear optical ferroelectric thin films for integrated photonic device applications should include:[142] (i) an application of experience gained from the integration of high-T_c superconductors and existing semiconductor technologies along with work on ferroelectric thin-film memory and dielectric applications; (ii) a study of existing single-crystal methods; (iii) optimization of thin-film deposition and characterization techniques; (iv) detailed analyses of thin-film microstructure and the influence of defect structures on optical properties; (v) identification of substrate/interlayer/waveguide epitaxial relationships novel device fabrication and integration strategies.

Roy et al.[143] have provided a comparison of common methods of ferroelectric thin-film preparation along with potential device applications (Table 6.1). A comparison of microstructure and composition variation evident in thin films deposited by various techniques was discussed. Thin-film microstructures (grain orientation, grain size, and porosity) were strongly influenced by the type of substrate, temperature, composition, and other processing parameters utilized. More importantly, the observed electrooptical properties can be correlated to thin-film microstructure. Issues such as ion bombardment and substrate temperature control need to be further studied for optimizing thin-film microstructure.[143] Roy et al. concluded that a more detailed understanding of processing microstructure relations was necessary for optimizing thin-film property control. Optimization of KTP thin-film processing for potential waveguide and photonic device fabrication is currently under investigation.[141]

6.2. Device Architecture and Design. The realization of integrated optic circuits depends on thin-film processing techniques for the fabrication of optical waveguides. Device applications are limited by ease of fabrication and integration, reproducibility, and the optical loss and damage threshold of the guide.[142] Current device architecture and design using KTP waveguides relies exclusively on single-crystal technology. However, limitations such as crystal size, complicated phase-matching schemes, and instabilities owing to complicated defect mechanisms, pose significant problems. Many of these problems could be avoided or alleviated by employing the novel design of photonic device structures based on KTP thin films. Applications such as miniature laser sources, optical data storage arrays and microscopic frequency doublers could be realized through utilizing integrated optical devices based on KTP thin films. It is expected that optical waveguides will be utilized in the near future with diode lasers to build compact visible light sources[144] that have practical applications in fiber optic communications, medicine, and optical computing. Work on the generation of UV and visible light in segmented KTP waveguides based on ion exchange has been completed by Laurell et al.[122] Phillips et al.[55] have examined the expansion of the optical window of KTP. Highly efficient Cherenkov-type SHG[145] and phase-matched

(142) Wood, V. E.; Swartz, S. L., unpublished work.
(143) Roy, R. A.; Etzold, K. F.; Cuomo, J. J. *Mater. Res. Soc. Symp. Proc.* **1990**, *200*, 141.
(144) Risk, W. P.; Lau, S. D.; Fontana, R.; Lane, L.; Nadler, C. *Appl. Phys. Lett.* **1993**, *63*, 1301.
(145) Doumuki, T.; Tamada, H.; Saitoh, M. *Appl. Phys. Lett.* **1994**, *64*, 3533.

Table 6.1. Comparison of Common Methods of Ferroelectric Thin-Film Preparation (After Roy et al.[143])

method	rate (Å/min)	epitaxy 1–10	stoichiometry 1–10	wet/dry	temp (°C) substrate	temp (°C) anneal	devices[a]	cost	miscellaneous problems
RF sputter	5–50	8	3	D	RT–700[b]	500–700	1–7	H	negative ions
magnetron sputter	50–300	5	5	D	RT–700	500–700	1–7	H	target surface
RF magnetron	50–100	9	5	D	RT–700	500–700	1–7	H	
ion beam sputter	20–100	9	8	D	RT–700	500–700	1–7	H	uniformity
evaporation	100–1000	7	4	D	RT–700	500–700	1–7	H	rate control
laser deposition	50–1000	9	6	D	RT–700	500–700	1, 3, 5	H	debris, uniformity
sol–gel	1000 Å/C	2–8	9	W	RT	450–800	1, 2, 3, 5	L	multiple coating
MOD	3000 Å/C	2	9	W	RT	500–800	1, 3, 5	L	high T_{anneal}
MOCVD	50–1000	5	7	D	400–800	600	1–6	H	high T_g

[a] The number scale for epitaxy and stoichiometry is: 1 (worst), 10 (best). Devices: (1) capacitor, (2) memory cell, (3) actuator, (4) electrooptic, (5) pyrodetector, (6) IR imager, and (7) SAW. [b] RT = room temperature.

SHG[146] in a Ta_2O_5/$KTiOPO_4$ waveguide configuration have also been achieved. Waveguide geometry and thin-film thickness strongly influenced the observed SHG conversion efficiency. Current research on the growth of KTP films by PELA focuses on the development of similar applications.[141] Thin-film fabrication offers a cost-effective strategy for the development of photonic devices along with enhanced design flexibility and capability. Research continues on the fabrication of NLO waveguides based on KTP thin films through the application of a more detailed understanding of the complex chemistry of this material.

7. Conclusions

KTP thin films offer a practical and cost-effective alternative to single crystals with enhanced design flexibility and capability for integrated optic applications. Owing to the continually expanding and versatile structure field of KTP, many opportunities exist for novel NLO thin-film fabrication not yet considered. Furthermore, problems such as size constraints and damage effects in single crystals could be solved through employing thin-film technologies. The need for complicated fluxes and elaborate high-temperature and high-pressure furnaces can be eliminated. It remains crucial to employ an understanding of the high-temperature chemistry of KTP in the fabrication of KTP thin films and photonic device structures. Any thin-film or waveguide processing technique which fails to recognize the complex chemistry of KTP will likely yield ineffective and inefficient devices. We must take advantage of the vast amount of information available on this outstanding NLO material. Through careful consideration of what is currently known regarding the KTP structure field, relevant defect chemistry, waveguide processing, and existing thin-film strategies, we have attempted to catalyze the use of high-quality KTP thin films for novel photonic applications.

A comparison of KTP thin films with other ferroelectric thin-film materials for photonic applications along with alternative thin-film deposition techniques such as metalloorganic chemical vapor deposition may prove important in the development of future integrated optical devices. Future challenges and perhaps a new agenda are emerging in materials chemistry. Laudise, a pioneering synthetic chemist, recently spoke on the new agenda and challenges of the materials chemist:[98] "Probably our greatest challenge is to insure a new generation of the best and the brighest in science, engineering, materials and chemistry. It should be the purpose of all of us in science and technology to convey the excitement, relevance and contributions of our activities." We hope that this review has indeed echoed this sentiment and look forward to the actualization of photonic devices based on KTP thin films.

Acknowledgment. We would like to thank the following individuals for their contributions: M. L. F. Phillips, V. E. Wood, M. T. Anderson, R. P. H. Chang, J. B. Ketterson, Fulin Xiong, P. M. Lundquist, C. A. Hijar, G. A. Taylor, and K. B. Greenwood. This work is supported by the MRL Program of the National Science Foundation, at the Materials Research Center of Northwestern University, under Award No. DMF-9120521.

CM940486G

(146) Doumuki, T.; Tamada, H.; Saitoh, M. *Appl. Phys. Lett.* **1994**, *65*, 2519.